Adaptive evolution in virulence effectors of the rice blast fungus *Pyricularia oryzae*

Marie LE NAOUR--VERNET[1]*, Florian CHARRIAT[1]*, Jérôme GRACY[2], Sandrine CROS-ARTEIL[1], Sébastien RAVEL[1,3], Florian VEILLET[1], Isabelle MEUSNIER[1], André PADILLA[2], Thomas KROJ[1], Stella CESARI[1]**, Pierre GLADIEUX[1]**

[1]PHIM Plant Health Institute, Univ Montpellier, INRAE, CIRAD, Institut Agro, IRD, Montpellier, France

[2]Centre de Biologie Structurale (CBS), Univ Montpellier, INSERM, CNRS, 29 rue de Navacelles, 34090 Montpellier, France.

[3]CIRAD, UMR PHIM, 34090 Montpellier, France

* These authors contributed equally to this work

** Corresponding authors:

Pierre Gladieux

Tel: +33 4 99 62 48 17

Email: pierre.gladieux@inrae.fr

Stella Cesari

Tel: +33 4 99 62 48 62

Email: stella.cesari@inrae.fr

Short title: MAX effector evolution in the rice blast fungus

ABSTRACT

Plant pathogens secrete proteins called effectors that target host cellular processes to promote disease. Recently, structural genomics has identified several families of fungal effectors that share a similar three-dimensional structure despite remarkably variable amino-acid sequences and surface properties. To explore the selective forces that underlie the sequence variability of structurally-analogous effectors, we focused on MAX effectors, a structural family of effectors that are major determinants of virulence in the rice blast fungus *Pyricularia oryzae*. Using structure-informed gene annotation, we identified 58 to 78 MAX effector genes per genome in a set of 120 isolates representing seven host-associated lineages. The expression of MAX effector genes was primarily restricted to the early biotrophic phase of infection and strongly influenced by the host plant. Pangenome analyses of MAX effectors demonstrated extensive presence/absence polymorphism and identified gene loss events possibly involved in host range adaptation. However, gene knock-in experiments did not reveal a strong effect on virulence phenotypes suggesting that other evolutionary mechanisms are the main drivers of MAX effector losses. MAX effectors displayed high levels of standing variation and high rates of non-synonymous substitutions, pointing to widespread positive selection shaping the molecular diversity of MAX effectors. The combination of these analyses with structural data revealed that positive selection acts mostly on residues located in particular structural elements and at specific positions. By providing a comprehensive catalog of amino acid polymorphism, and by identifying the structural determinants of the sequence diversity, our work will inform future studies aimed at elucidating the function and mode of action of MAX effectors.

AUTHOR SUMMARY

Fungal plant pathogens use small secreted proteins, called effectors, to manipulate to their own advantage their host's physiology and immunity. The evolution of these effectors, whether spontaneously or in response to human actions, can lead to epidemics or the emergence of new diseases. It is therefore crucial to understand the mechanisms underlying this evolution. In this article, we report on the evolution of effectors in one of the prime experimental model systems of plant pathology, *Pyricularia oryzae*, the fungus causing blast diseases in rice, wheat, and other cereals or grasses. We further characterize in this fungus a particular class of effectors, called MAX effectors, using structural models based on experimental protein structures of effectors. We show that this class of effector is produced by the pathogen during the early stages of infection, when plant cells are still alive. By comparing the gene content of isolates infecting different plant species, we show that the MAX effector arsenal is highly variable from one isolate to another. Finally, using the inferential framework of population genetics, we demonstrate that MAX effectors exhibit very high genetic variability and that this results from the action of natural selection.

66 **INTRODUCTION**

67 Plant pathogens secrete effector proteins to manipulate the physiology and metabolism of their
68 host and to suppress its immunity. Consequently, effectors are expected to engage in
69 coevolutionary interactions with plant defense molecules. The proximate mechanisms of
70 effector-driven adaptation are relatively well-characterized: plant pathogens adapt to new hosts
71 through changes in effector repertoires and effector sequences [1, 2]. However, the ultimate
72 (eco-evolutionary) mechanisms underlying effector diversification have remained elusive. The
73 concept of coevolution posits that adaptation in one partner drives counter-adaptations in the
74 coevolving partner [3-5]. Under the co-evolutionary arms race model, variation for disease
75 resistance and pathogen virulence is transient, resulting in a turnover of sequence variation
76 through repeated episodes of strong directional selection [6]. In agricultural systems, because
77 pathogens tend to be ahead of their hosts in the arms race owing to their larger populations and
78 shorter generation times, the co-evolutionary arms race tends to result in so-called boom and
79 bust cycles [7]. Under the alternative, 'trench warfare' hypothesis, advances and retreats of
80 resistance or virulence genes frequencies maintain variation as dynamic polymorphisms [8, 9].
81 The maintenance of genetic polymorphisms is called 'balancing selection', a process by which
82 different alleles or haplotypes are favored in different places (via population subdivision)
83 and/or different times (via frequency-dependent negative selection). While there is a growing
84 body of data demonstrating the nature and prevalence of the selective pressures that shape the
85 diversity of immune systems in plants [6, 10-12], we still lack a clear picture of the co-
86 evolutionary mechanisms underlying the molecular evolution of virulence factors in their
87 interacting antagonists [13].

88 Effectors from plant pathogenic fungi are typically cysteine-rich secreted proteins
89 smaller than 200 amino acids with an infection-specific expression pattern. Effectors are
90 numerous in fungal genomes (several hundred to more than a thousand per genome), and rarely
91 show homologies with known proteins or domains. They are also highly variable in sequence
92 and do not form large families of sequence homologs. Based on similarity analyses, fungal

effectors can form small groups of paralogs (typically with less than five members), but they are most often singletons. This apparent lack of larger effector families has hindered attempts to probe into the evolutionary factors underlying their diversification. In addition, the high diversity of fungal effectors has hampered functional analyses due to the lack of good criteria for prioritizing them and our inability to predict their physiological role. Consequently, the virulence function and evolutionary history of most fungal effectors remain unknown.

Recently, the resolution of the three-dimensional (3D) structure of fungal effectors combined with Hidden Markov Model (HMM) pattern searches and structure modeling revealed that fungal effector repertoires are, despite their hyper-variability, dominated by a limited number of families gathering highly sequence-diverse proteins with shared structures and, presumably, common ancestry [14-17]. One such structurally-conserved but sequence-diverse fungal effector family is the MAX (*Magnaporthe* Avrs and ToxB-like) effector family. MAX effectors are specific to ascomycete fungi and show massive expansion in *Pyricularia oryzae* (synonym: *Magnaporthe oryzae*) [17], the fungus causing rice blast disease, one of the most damaging diseases of rice [18, 19]. MAX effectors are characterized by a conserved structure composed of six β-strands organized into two antiparallel β-sheets that are stabilized in most cases by one or two disulfide bridges. The amino acid sequence of MAX effectors is very diverse and they generally have less than 15% identity, which suggests that they are a family of analogous, rather than homologous, effector proteins. In other words, they share a similar three-dimensional structure, but no conclusions can be drawn with respect to shared ancestry. MAX effectors are massively expressed during the biotrophic phase of infection, suggesting an important role in disease development and fungal virulence [17]. Remarkably, about 50% of the known avirulence (AVR) effectors of *P. oryzae* belong to the MAX family, indicating that these effectors are closely monitored by the host plant immune system [17].

Pyricularia oryzae is a multi-host, poly-specialist pathogen that infects more than 50 monocotyledonous plants, including major cereal crops such as rice, maize, wheat, or barley [20-23]. *Pyricularia oryzae* has repeatedly emerged on new hosts [21, 24], in new geographical areas

120 [25, 26], and phylogenomic analyses have revealed that it can be subdivided into several genetic
121 lineages, each preferentially associated with a specific or restricted set of host plant genera [27].
122 In *P. oryzae*, effectors can play a major role in host-shifts or host-range expansions [28-30]. For
123 example, loss of function of the PWT3 effector in *Lolium*-infecting strains contributed to gain of
124 virulence on wheat [29]. Similarly, loss of the MAX effector AVR1-CO39 is thought to have
125 contributed to the emergence of rice blast from foxtail-millet infecting isolates [20, 31]. This
126 indicates that MAX effectors may be important determinants of host specificity in *P. oryzae*.

127 In this study, we characterized the genetic diversity of MAX effectors in *P. oryzae* and
128 within its different host-specific lineages. We explored the evolutionary drivers of the
129 diversification of MAX effectors and tested whether MAX effectors represent important
130 determinants of *P. oryzae* host specificity. To this aim, we assembled and annotated 120 high-
131 quality *P. oryzae* genomes from isolates representing seven main host-specific lineages. We
132 mined these genomes for putative effectors and used hidden Markov models based on fold-
133 informed protein alignments to annotate putative MAX effectors. We identified 58 to 78 putative
134 MAX effector genes per individual genome distributed in 80 different groups of MAX homologs.
135 We showed that the expression of *MAX* effector genes is largely restricted to the early biotrophic
136 phase of infection and strongly influenced by the host plant. Our evolutionary analyses showed
137 that MAX effectors harbor more standing genetic variation than other secreted proteins and
138 non-effector genes, and high rates of non-synonymous substitutions, pointing to positive
139 selection as a potent evolutionary force shaping their sequence diversity. Pangenome analyses of
140 MAX effectors demonstrated extensive presence/absence polymorphism and identified several
141 candidate gene loss events possibly involved in host range adaptation. Our work demonstrates
142 that MAX effectors represent a highly dynamic compartment of the genome of *P. oryzae*, likely
143 reflecting intense co-evolutionary interactions with host molecules.

144 **RESULTS**

145 *Genome assembly and prediction of MAX effector genes.*

146 We used a collection of genome assemblies that included 120 haploid isolates of *Pyricularia*
147 *oryzae* fungi from 14 different host genera: *Oryza* (n=52), *Triticum* (n=21), *Lolium* (n=12),
148 *Setaria* (n=8), *Eleusine* (n=8), *Echinochloa* (n=4), *Zea* (n=4), *Bromus* (n=2), *Brachiaria* (n=2),
149 *Festuca* (n=2), *Stenotaphrum* (n=2), *Eragrostis* (n=1), *Hordeum* (n=1), and *Avena* (n=1) (S1
150 Table). Assembly size ranged from 37Mb to 43.2Mb, with an average size of 40.2 Mb (standard
151 deviation [s.d.]: 1.9Mb). L50 ranged from five to 411 contigs (mean: 97.1; s.d.: 83.2) and N50
152 from 28Kb to 4.0Mb (mean: 238.6Kb; s.d.: 43.8Kb; S1 Table). Gene prediction based on protein
153 sequences from reference 70-15 and RNAseq data identified 11,520 to 12,055 genes per isolate
154 (mean: 11,763.2; s.d.: 103.7). The completeness of assemblies, as estimated using BUSCO [32],
155 ranged between 93.4 and 97.0% (mean: 96.4%; s.d.: 0.6%; S1 Table).

156 MAX effectors were identified among predicted secreted proteins using a combination of
157 similarity searches [33, 34] and structure-guided alignments [35] as summarized in Figure 1. To
158 assess variation in the MAX effector content of *P. oryzae*, we constructed groups of homologous
159 genes (i.e., "orthogroups" or OG) using the clustering algorithm implemented in ORTHOFINDER
160 [36]. A given orthogroup was classified as secreted proteins or MAX effectors if 10% of
161 sequences in the group were identified as such by functional annotation. Sequences were
162 grouped in 14,767 orthogroups, of which 80 were classified as encoding MAX effectors and
163 3,283 as encoding other types of secreted proteins (Figure 1). The number of MAX orthogroups
164 per isolate ranged from 58 to 73 (average: 65.8; s.d.: 2.8), representing between 58 to 78 *MAX*
165 genes per isolate (average: 68.4; s.d.: 3.6). The 80 orthogroups of MAX effectors were further
166 split into 94 groups of orthologs, by identifying paralogs using gene genealogies inferred with
167 RAxML v8 [37] (S2 Table). Comparison of these 94 groups of orthologs with MAX effectors
168 predicted by previous studies [15-17, 38] revealed that 19 were not predicted by any other
169 study, while 75 were predicted by at least one other study (including nine predicted by all

170 studies). Twenty-five MAX effectors predicted by other analyses, were not identified by our
171 prediction pipeline and were, therefore, not considered in our study (S2 Table).

172 The number of MAX effectors per isolate was primarily determined by the host of origin.
173 We did not observe any significant relationship between the number of MAX effectors and
174 assembly properties (assembly size and N50), unlike the number of secreted proteins and total
175 number of genes (S1 Figure). Analysis of variance revealed that the host of origin had a
176 significant impact on the number of MAX effectors ($F_{13,95}$=10.33; p=3e^{-8}), while the origin of
177 genomic data did not have an effect (i.e., the study in which genomic data were initially
178 described; $F_{11,95}$=1.07; p=0.39; S1 Figure). These analyses indicate that the observed variation
179 in the size of the MAX effector repertoire is primarily biological in origin, not technical.
180

181 *MAX effectors are massively deployed during rice infection.*

182 To determine whether these putative MAX effectors are deployed by *P. oryzae* during plant
183 infection, we analyzed the expression patterns of the 67 *MAX* genes predicted in the genome of
184 the reference isolate Guy11 by qRT-PCR (Figure 2A). Using RNA samples from Guy11 mycelium
185 grown on artificial media, we found that 94% of the *MAX* genes (63 genes) were not, or very
186 weakly expressed during axenic culture, and only four (i.e., *MAX24*, *MAX29, MAX59,* and
187 *MAX66*) showed weak, medium or strong constitutive expression (Figure 2A). *MAX* genes were,
188 therefore, predominantly repressed in the mycelium of *P. oryzae*.

189 We analyzed the expression of the *MAX* genes 2, 3, 4, and 7 days following spray
190 inoculation of Guy11 on the rice cultivar Maratelli, which is highly susceptible to *P. oryzae*. We
191 found that 67% of the *MAX* genes (45 genes) were expressed (Figure 2A). Among them, three
192 were also expressed in the mycelium (i.e., *MAX31, MAX59*, and *MAX94*). *MAX31* was over-
193 expressed under infection conditions, whereas the other two showed similar expression levels
194 *in vitro* and during infection. 64% of the *MAX* genes (42 genes) showed an infection-specific
195 expression profile with relative expression levels ranging from very low (0.008-0.04) to very
196 high (>5). Like the *Bas3* gene, encoding a *P. oryzae* effector specifically induced during the

197 biotrophic phase of infection, all *MAX* genes showed maximal expression between the second
198 and fourth day post-inoculation (Figure 2A; S2 Figure).

199 To test whether the genotype of the host plant could influence the expression of *MAX*
200 genes, we analyzed their expression patterns upon infection of the rice cultivar Kitaake, which
201 has a higher basal resistance to *P. oryzae* than Maratelli. We computed the median relative
202 expression across three independent experiments with five biological replicates each (Figure
203 2A; Figure 2B). During Kitaake infection, 78% of the *MAX* genes (52 genes) were upregulated
204 compared to the *in vitro* condition, while 64% (43 genes) were induced upon infection of
205 Maratelli (Figure 2A). Some *MAX* genes not expressed in Maratelli were induced in Kitaake (e.g.,
206 *MAX24, MAX30, MAX32, MAX43, MAX71,* and *MAX73*) (Figure 2B, S3 Figure). Others were
207 significantly upregulated in Kitaake compared to Maratelli (i.e., *MAX22, MAX44, MAX55, MAX57,*
208 *MAX69*, and *MAX91*). However, a few genes, such as *MAX15, MAX37* and *MAX62*, among the
209 most strongly expressed effectors in Maratelli, showed weaker levels of expression in Kitaake.
210 These results show that Guy11 deploys a wider diversity of MAX effectors during the infection of
211 Kitaake compared to that of Maratelli, and that MAX effectors are subject to host-dependent
212 expression polymorphism.

213 Taken together, our data indicate that during the biotrophic phase of rice infection, *P.*
214 *oryzae* actively expresses a significant portion of its MAX effector repertoire in a host-dependent
215 manner, which suggests that these effectors have an important function in fungal virulence.

216

217 *The MAX effector repertoire is highly variable.*

218 To investigate the genetic diversity of MAX effectors in *P. oryzae*, we analyzed their nucleotide
219 diversity per base pair (π), their ratio of non-synonymous to synonymous nucleotide diversity
220 (π_N/π_S; page 226 in ref. [39]), and their presence-absence polymorphism. Compared to other
221 secreted proteins or other genes, MAX effector orthogroups had higher π, and π_N/π_S values, and
222 lower presence frequency (S4 Figure). Orthogroups including known avirulence genes like

223 *AVR1-CO39*, *AvrPiz-t* and *AVR-Pik* featured among the most diverse orthogroups of MAX
224 effectors (S1 Data).

225 We categorized genes in the pangenome according to their presence frequencies [36],
226 with core genes present in all isolates, softcore genes present in >99% isolates, shell genes
227 present in 1-99% isolates and cloud genes present in <1% isolates. The majority of MAX effector
228 genes were classified as shell (64/80 [80%] orthogroups), while the majority of other secreted
229 proteins or other genes were classified as core or softcore (1650/3283 [50.2%] and
230 6714/11404 [58.9%] orthogroups, respectively) (Figure 3A). Only a minority of genes were
231 present in multiple copies (MAX: 15/80 [18.8%]; other effectors: 746/3283 [22.7%]; other
232 genes: 1439/11404 [12.6%]; Figure 3A). Assessment of the openness of the pan-genome by
233 iteratively subsampling isolates revealed a closed pangenome with a limited number of pan and
234 core genes for MAX effectors, other secreted proteins and the remainder of the gene space
235 (Figure 3B). Nucleotide diversity differed significantly between categories of the pangenome for
236 non-MAX effectors (Kruskal-Wallis test: H=181.17, d.f.=2, $p<0.001$) and other genes (Kruskal-
237 Wallis test: H=225.25, d.f.=2, $p<0.001$), but not for MAX effectors (Kruskal-Wallis test: H=2.50,
238 d.f.=2, $p>0.05$). For non-MAX effectors and other genes, nucleotide diversity π was significantly
239 higher in the shell genes than in softcore genes and core genes (Post-hoc Mann-Whitney U-tests,
240 $p<0.001$; Figure 3C). The frequency of MAX orthogroups was positively and significantly
241 correlated with the frequency of neighboring orthogroups at the species-wide level and at the
242 level of Oryza and Setaria lineages, which indicates that non-core MAX effectors tend to be
243 located in regions with presence-absence variation (S5 Figure).

244 Together, these analyses show that the MAX effector repertoire is highly plastic
245 compared to other gene categories, both in terms of the presence/absence of orthogroups and
246 the sequence variability within orthogroups.

247
248 *MAX effector variability is structured by host plant.*

249 To investigate signatures of positive selection in the genome of *P. oryzae*, and identify candidate
250 loci involved in host specificity, we first identified the divergent lineages represented in our

251 dataset. We inferred population structure from 6780 SNPs in single-copy core orthologs to
252 minimize the potential impact of natural selection on our findings. We used complementary
253 approaches that make no assumption about random mating or linkage equilibrium. Both
254 clustering analyses with the sNMF software [40] (Figure 4A) and neighbor-net phylogenetic
255 networks [41] (Figure 4B) revealed consistent patterns that split genetic variation primarily by
256 host of origin. Although the lowest cross-entropy value was observed at K=11 in the sNMF
257 analysis, we chose to represent K=8 because the cross-entropy was only slightly higher and K=8
258 did not split the *Triticum*- and *Eleusine*-associated clusters (S6 Figure). Lineage-level analyses
259 were limited to the lineages with the largest sample size, associated with rice (*Oryza*), foxtail
260 millet (*Setaria*), wheat (*Triticum*), ryegrass (*Lolium*), and goosegrass (*Eleusine*).

261 Population subdivision inferred from MAX effectors using either 130 SNPs without
262 missing data in single-copy core MAX effectors (Figure 4C) or presence/absence variation of all
263 80 MAX effector orthogroups (Figure 4D) revealed essentially the same groups as the analysis of
264 the single-copy core orthologs. This indicates that genome-wide nucleotide variation, variation
265 in MAX effector content, and nucleotide variation at MAX effectors reflected similar genealogical
266 processes. The *Oryza* and *Setaria* lineages displayed exceptionally high presence/absence
267 variation of MAX effectors (average Hamming distance between pairs of isolates: 0.123 and
268 0.095; Figure 4D), but only limited sequence variation at single-copy core MAX effectors
269 (average Hamming distance between pairs of isolates: 0.017 and 0.012; Mann-Whitney U-tests,
270 $p<0.05$; Figure 4C).

271
272 *Loss of MAX effectors in specific lineages does not appear to be associated with host specificity.*

273 The comparison of the MAX effector content in the genomes of 120 *P. oryzae* isolates revealed
274 extensive presence/absence polymorphism between host-specific groups (S3 Table). To address
275 the underlying evolutionary mechanisms, we tested experimentally the hypothesis that MAX
276 effector losses are massively related to escape from receptor-mediated non-host resistance.
277 Indeed, the loss of MAX effectors in specific lineages of *P. oryzae* could primarily serve to escape
278 from non-host resistance during infections of novel plant species carrying immune receptors

279 specifically recognizing these effectors. To test this hypothesis, we focused on the *Oryza*- and
280 *Setaria*-infecting lineages, as previous investigations suggested that the *Oryza*-infecting lineage
281 emerged by a host shift from *Setaria* and we found both groups to be closely related (Figure 4)
282 [21, 42]. Our strategy was to introduce into the *Oryza*-isolate Guy11 MAX effectors absent from
283 the *Oryza* lineage but present in the *Setaria* lineage, and to assess the ability of these transgenic
284 isolates to infect rice.

285 We identified three MAX orthogroups that were largely or completely absent from the
286 *Oryza* lineage, but present in the majority of isolates of the other lineages (S3 Table).
287 Orthogroup MAX79 (OG0011591-1) was absent in all 52 *Oryza*-infecting isolates, while MAX83
288 (OG0011907), and MAX89 (OG0012141) were absent in 50 and 46 of them, respectively (S3
289 Table). Constructs carrying the genomic sequence of *MAX79*, *MAX83* or *MAX89* derived from the
290 *Setaria* isolate US0071 and under the control of the strong infection specific promoter of the
291 effector *AVR-Pia* were generated and stably introduced into Guy11. For each construct, three
292 independent transgenic lines were selected. Transgene insertion was verified by PCR and the
293 expression of transgenes was measured by qRT-PCR (S7 Figure). To test whether the selected
294 MAX effectors trigger immunity in rice, the transgenic isolates were spray-inoculated onto a
295 panel of 22 cultivars representative of the worldwide diversity of rice (S4 Table).

296 As controls, we used the MAX effectors *AVR-Pia*, which is rare outside the *Oryza* and
297 *Setaria* lineages, and *AVR1-CO39*, which is absent or pseudogenized in the *Oryza* lineage, but
298 present in all other host-specific lineages including *Setaria*. Both effectors are detected in rice by
299 the paired NLR immune receptors RGA4 and RGA5 from the *Pi-a/Pi-CO39* locus and thereby
300 contribute, respectively, to host or non-host resistance in this plant species [43, 44].

301 As expected, isolates expressing *AVR1-CO39* or *AVR-Pia* triggered resistance in the rice
302 variety Aichi Asahi that carries *Pi-a*, but caused disease on Nipponbare (*pi-a*$^-$) and other varieties
303 lacking this *R* locus (Figure 5; S4 Table). Unlike the positive controls, the effectors MAX79,
304 MAX83 and MAX89 were not recognized and did not induce resistance in any of the tested rice
305 cultivars (Figure 5; S4 Table). The disease symptoms caused by the transgenic isolates carrying

306 these effectors were similar to those observed for wild-type Guy11 or Guy11 isolates carrying an
307 *RFP* (red fluorescent protein) construct. This suggests that these effectors do not significantly
308 increase the virulence of Guy11.

309 These experiments show that despite their loss in the *Oryza*-infecting lineage of *P.*
310 *oryzae,* and unlike AVR1-CO39, the effectors MAX79, MAX83, and MAX89 do not seem to induce
311 non-host resistance in rice. Consequently, other mechanisms than escape from host immunity
312 contributed to the loss of these MAX effectors during the putative host shift of *P. oryzae* from
313 *Setaria* to *Oryza*.

314

315 *MAX effectors display signatures of balancing selection.*

316 To investigate the impact of balancing selection on MAX effector evolution, we focused on single-
317 copy core, softcore, and shell orthogroups to avoid the possible effect of gene paralogy. We then
318 computed π (nucleotide diversity per bp), F_{ST} (the amount of differentiation among lineages
319 [45]), π_N (non-synonymous nucleotide diversity), π_S (synonymous nucleotide diversity), and
320 π_N/π_S (the ratio of non-synonymous to synonymous nucleotide diversity). Large values of π and
321 π_N/π_S, in particular, are possible indicators of a gene being under balancing selection.

322 Nucleotide diversity (π) differed significantly between groups of genes (Kruskal-Wallis
323 test, H=509.9, d.f.=2, p <0.001; Figure 6A; S5 Table). π was significantly higher for the set of
324 MAX effectors (average π: 0.0104, standard deviation: 0.0137), than for other secreted proteins
325 (average π: 0.0079, standard deviation: 0.020), and other genes (average π: 0.0049, standard
326 deviation: 0.014; Mann-Whitney U-tests, p<0.05), showing that MAX effectors, and to a smaller
327 extent other secreted proteins, are more variable than a typical gene. At the lineage level,
328 however, nucleotide diversity at MAX effectors tended to not significantly differ from other
329 putative effectors, or other genes (S5 Table).

330 In addition to having greater nucleotide variation than other genes at the species level,
331 MAX effectors also displayed a higher ratio of non-synonymous to synonymous nucleotide
332 diversity (Figure 6B; S5 Table). The π_N/π_S ratio differed significantly between groups of genes

333 (Kruskal-Wallis tests H=101.4, $d.f.$=2, p<0.001), and the excess of non-synonymous diversity
334 was significantly, and markedly, higher for MAX effectors (average π_N/π_S: 1.826, standard
335 deviation: 3.847) than for other effectors (average π_N/π_S: 0.461, standard deviation: 1.600), and
336 other genes (average π_N/π_S: 0.448, standard deviation: 1.463; Mann-Whitney U-tests, p<0.05).
337 The higher π_N/π_S of MAX effectors was mostly driven by differences in π_N (Figure 6A; S5 Table).
338 Twenty MAX effectors displayed values in the top 5% percentile of non-effector genes, far
339 exceeding the four genes expected by chance (p<0.05). More specifically, 26 MAX effectors
340 displayed π_N/π_S values greater than 1, which is the value expected under neutrality. This
341 included three well-known avirulence genes: *AVR1-CO39* (π_N/π_S=2.564), *AVR-Pik*
342 (π_N/π_S=15.574), and *AvrPiz-t* (π_N/π_S=1.431). The average π_N/π_S ratio was also higher at MAX
343 effectors than other secreted proteins and other genes in all lineages, with significant differences
344 in four lineages (Mann-Whitney U-tests, p<0.05), and the average π_N/π_S was greater than one in
345 the *Oryza* lineage (Figure 6B; S5 Table). Seven to eleven MAX effectors had $\pi_N/\pi s$>1 at the
346 lineage level, representing 8% (*Setaria*-infecting lineage) to 41% (*Lolium*-infecting lineage) of
347 MAX effectors with a defined $\pi_N/\pi s$ ratio (S2 Data).

348 π_N/π_S>1 is a strong indication of multiallelic balancing selection (*i.e.*, multiple alleles at
349 multiple sites are balanced), as single sites under very strong balancing selection cannot
350 contribute enough non-synonymous variability to push the π_N/π_S ratio above one [46]. To assess
351 whether the adaptation of lineages to their respective hosts may contribute to the species-wide
352 excess of non-synonymous diversity detected at MAX effectors, we estimated population
353 differentiation. The differentiation statistic F_{ST} differed significantly between groups of genes
354 (Kruskal-Wallis tests H=8.731, $d.f.$=2, p=0.013), and differentiation was significantly higher for
355 MAX effectors than for other secreted proteins and other genes (Figure 6A; S5 Table). F_{ST} was
356 also significantly, albeit relatively weakly, correlated with π_N/π_S at MAX effectors (Spearman's ρ:
357 0.304, p=0.007; S8 Figure). These observations indicate that between-lineages differences in
358 allele frequencies are greater for MAX effectors than for other secreted proteins or other genes,
359 which may result from divergent selection exerted by hosts.

360

361 *MAX effectors display signatures of recurrent directional selection.*

362 To detect adaptive molecular evolution, we collected orthologous sequences from outgroup
363 *Pyricularia sp.* LS [47, 48] and estimated the d_N/d_S ratio (the ratio of non-synonymous to
364 synonymous substitution rates) using a maximum likelihood method [49]. Note that d_N/d_S was
365 not computed at the intra-specific level, but computed along the branches connecting the
366 outgroup and isolates from the ingroup. Outgroup sequences could be retrieved for 10,174 out
367 of 14,664 single-copy orthogroups, including 66 out of 94 single-copy orthologs of MAX
368 effectors. The d_N/d_S ratio differed significantly between groups of genes (Kruskal-Walli. s tests
369 H=45.812, $d.f.$=2, p<0.001; Figure 6A; S5 Table), and was higher for MAX effectors (average
370 d_N/d_S: 0.977, s.d.: 1.316) than for other secreted proteins (average d_N/d_S: 0.711, s.d.: 1.722), and
371 other genes (average d_N/d_S: 0.584, s.d.: 1.584; Mann-Whitney U-tests, p<0.05). The same pattern
372 of higher d_N/d_S for MAX effectors was observed at the lineage level (S5 Table). Twenty-four of
373 the 66 MAX effectors with outgroup sequence (i.e., 36.4%) showed d_N/d_S>1 (S2 Data), which is a
374 strong indication of directional selection. d_N/d_S>1 is only expected for genes that have
375 experienced repeated bouts of directional selection which led to repeated fixations of amino-
376 acid substitutions [46]. Eleven MAX effectors displayed signatures of both multiallelic balancing
377 selection (π_N/π_S>1) and multiallelic directional selection (d_N/d_S>1).

378 The divergence data, therefore, indicate that a scenario of molecular co-evolution
379 involving repeated selective sweeps may apply to a substantial fraction (at least one-third) of
380 MAX effectors.

381

382 *Structural determinants of polymorphism and divergence at MAX effectors.*

383 Different parts of proteins can be under different selective forces. To investigate if this is the
384 case in MAX effectors, we examined the relationship between three different measures of
385 diversity and three structural features. The measures of diversity were (1) the probability of an
386 amino acid being polymorphic, (2) the non-synonymous nucleotide diversity π_N, and (3) the

387 d_N/d_Sratio. The analyzed structural features were: (1) secondary structure annotations with the
388 three subclasses "extended conformation", "coils", and "turns"; (2) solvent accessibility
389 percentage of the Van der Waals surface of the amino acid side chain, with the three sub-classes:
390 0-30% (buried), 30-60% (intermediate), and 60-100% (exposed); (3) structural domains, with
391 six subclasses that grouped the coil, extended conformation and turn residues that define the six
392 beta strands characteristic of MAX effectors. Structural features were determined using MAX
393 effector structures predicted by homology modeling and computing with STRIDE.

394 For the relationship between the probability of residues being polymorphic and the
395 structural features, we used a generalized linear mixed model with a set of predictor variables.
396 The fixed effects were the structural features and the model was fitted using maximum
397 likelihood estimation, with MAX effector modeled as a random effect. Only a single structural
398 feature, the solvent accessibility had a statistically significant effect on the probability of amino
399 acid polymorphism (S1 Text). Predicted probabilities of amino acid change were higher for
400 accessibility class 60-100% (95% prediction interval: 0.1294-0.1295), than for accessibility
401 classes 30-60% (95% prediction interval: 0.1029-0.1049) and 0-30% (95% prediction interval:
402 0.0834-0.0835). A major factor explaining the variability of the response variable turned out to
403 be the identity of MAX effectors. Indeed, the random effect (σ: 1.17) had a larger standard
404 deviation than the largest fixed-effect factor (coefficient for accessibility class 60-100%: 0.64)
405 (S1 Text).

406 To visualize the localization of polymorphisms, we projected the distribution of amino
407 acid changes on the surface of protein structure models of two types of MAX effectors: those
408 with an avirulence function and MAX effectors with the strongest signatures of multiallelic
409 balancing selection (π_N/π_S>2; Figure 6C; S9 Figure). For the three effectors whose binding
410 interfaces have been experimentally characterized (AVR1-CO39, AVR-Pia, AVR-Pik [50-53]), a
411 substantial fraction of amino acid changes co-localized with residues interacting with immune
412 receptors and, presumably, also with their host target proteins. Polymorphic residues are,
413 therefore, potentially good predictors for binding interfaces in MAX effectors and the specific

414 surface regions, where polymorphisms cluster in several MAX effectors (such as MoToxB,
415 MAX58, MAX87, MAX69, or MAX50) could correspond to interfaces that bind immune receptors
416 and/or host target proteins (Figure 6C).

417 To determine which parts of the MAX structure is most responsible for the high level of
418 standing variation in these effectors, we calculated for the three different structural features and
419 their subclasses the non-synonymous nucleotide diversity π_N (S10 Figure). We restricted this
420 analysis to the 25 MAX effectors exhibiting balancing selection ($\pi_N/\pi_S > 1$) and we used π_N and
421 not π_N/π_S because the latter tended to be undefined due to relatively short sequence lengths.
422 Non-synonymous nucleotide diversity π_N differed between subclasses (Kruskal-Wallis tests
423 H=8.504, $d.f.$=2, p=0.014; Figure 6D; S6 Table) and was higher at coils and turns, than at
424 extended conformations (coils: π_N=0.0191; turns: π_N=0.0167; extended conformations:
425 π_N=0.0086; posthoc Mann-Whitney U-tests, $p<0.05$). Ten and nine MAX effectors displayed
426 their highest values of π_N in coils and turns, respectively. π_N did not significantly differ between
427 relative solvent accessibility subclasses (Kruskal-Wallis tests H=2.308, $d.f.$=2, p=0.315), but
428 differences were marginally significant between structural domains (Kruskal-Wallis tests
429 H=11.035, $d.f.$=5, p=0.051). The third, fourth, and fifth beta strands displayed the highest levels
430 of non-synonymous diversity (π_N=0.0341, π_N=0.0341, and π_N=0.0341, respectively), and 18 out
431 of 25 MAX effectors displayed their highest values of π_N at one of these three beta strands (S6
432 Table).

433 To identify the parts of MAX effector structures that experience multiallelic directional
434 selection, we analyzed the 23 proteins with $d_N/d_S > 1$. This showed that differences in d_N/d_S were
435 most pronounced between subclasses of structural features (Kruskal-Wallis tests H=5.499,
436 $d.f.$=2, p=0.064), with higher average d_N/d_S values for coils and turns (d_N/d_S=2.490 and
437 d_N/d_S=1.184, respectively) than extended conformations (d_N/d_S=0.573) (Figure 6E; S6 Table).
438 The average d_N/d_S was also close to one for the 30-60% subclass of relative solvent accessibility
439 (d_N/d_S=0.994), and 12 MAX effectors with signatures of directional selection had their highest
440 d_N/d_S values for this subclass, although differences were not significant.

441 Overall, these analyses show that multiallelic balancing and directional selection acted
442 preferentially on coils and turns, but that the impact of two forms of selection on structural
443 domains and solvent accessibility subclasses differs.
444
445 **DISCUSSION**
446 *MAX effectors as model systems to investigate effector evolution.*
447 Effectors involved in coevolutionary interactions with host-derived molecules are expected to
448 undergo non-neutral evolution. Yet, the role of natural selection in shaping polymorphism and
449 divergence at effectors has remained largely elusive [2]. Despite the prediction of large and
450 molecularly diversified repertoires of effector genes in many fungal genomes, attempts to probe
451 into the evolutionary drivers of effector diversification in plant pathogenic fungi have been
452 hindered by the fact that, until recently, no large effector families had been identified. In this
453 study, we overcome the methodological and conceptual barrier imposed by effector hyper-
454 diversity by building on our previous discovery [17] of an important, structurally-similar, but
455 sequence-diverse family of fungal effectors called MAX. We used a combination of structural
456 modeling, evolutionary analyses, and molecular plant pathology experiments to provide a
457 comprehensive overview of polymorphism, divergence, gene expression, and presence/absence
458 at MAX effectors. When analyzed species-wide or at the level of sub-specific lineages, ratios of
459 non-synonymous to synonymous nucleotide diversity, as well as ratios of non-synonymous to
460 synonymous substitutions, were consistently higher at MAX effectors than at other loci. At the
461 species level, the two ratios were also significantly higher than expected under the standard
462 neutral model for a large fraction of MAX effectors. The signatures of adaptive evolution
463 detected at MAX effectors, combined with their extensive presence/absence variation, are
464 consistent with their central role in coevolutionary interactions with host-derived ligands that
465 impose strong selection on virulence effectors.
466
467 *Adaptive evolution of MAX effectors*

468 Rates of evolution determined from orthologous comparisons with outgroup sequences revealed
469 that, for a large fraction of MAX effectors, non-synonymous changes have accumulated faster
470 than synonymous changes. The fast rate of amino-acid change at MAX effectors is consistent
471 with a classic arms race scenario, which entails a series of selective sweeps as new virulent
472 haplotypes - capable of avoiding recognition by plant immune receptors that previously
473 prevented pathogen multiplication - spread to high frequency [54, 55]. Furthermore, it is
474 important to note that although large values of the d_N/d_S ratio provide strong evidence for
475 directional selection, small values do not necessarily indicate the lack thereof, as d_N/d_S ratios
476 represent the integration of genetic drift, constraint, and adaptive evolution [50][56]. Much of
477 the adaptive changes at MAX effectors probably took place before the radiation of *P. oryzae* on
478 its various hosts. However, the observation that d_N/d_S values determined from orthologous
479 comparisons with outgroup are higher at the species level than at the sub-specific lineage level
480 indicates that part of the signal of directional selection derives from inter-lineage amino acid
481 differences associated with host-specialization. Our structural modeling indicates that it is
482 preferentially "turns" and "coils", but also residues with intermediate solvent accessibility,
483 which often evolve at an unusually fast rate, and therefore that these are probably the residues
484 of MAX proteins preferentially involved in coevolutionary interactions with host-derived
485 molecules.

486 MAX effectors are characterized by a remarkable excess of non-synonymous
487 polymorphism, compared to synonymous polymorphism, at the species level, but also - albeit to
488 a lesser extent - at the sub-specific lineage level. This raises the question of how polymorphisms
489 are maintained in the face of adaptive evolution, given that selective sweeps under a classic arms
490 race scenario are expected to erase variation [6, 9]. Directional selection restricted to host-
491 specific lineages - i.e., local adaptation - may contribute to the signature of multiallelic balancing
492 selection observed at the species level. The observation of a positive correlation between π_N/π_S
493 and the differentiation statistic F_{ST}, together with the fact that most MAX effectors are
494 monomorphic at the lineage level, are consistent with a role of divergent selection exerted by

495 hosts in the maintenance of species-wide diversity at MAX effectors. However, the finding that
496 MAX effectors with a defined π_N/π_S at the sub-specific lineage level (i.e., MAX effectors with
497 $\pi_S \neq 0$) present a higher ratio than the other genes also indicates that the adaptive evolution
498 process is not simply one of successive selective sweeps. This is consistent with balancing
499 selection acting at the lineage level, through which polymorphisms in MAX virulence effectors
500 are maintained due to spatiotemporal variation in selection pressures posed by the hosts – a
501 process known as the trench-warfare model [54]. MAX effectors can experience varying
502 selection pressures due to differences in both arsenals of immune receptors and repertoires of
503 virulence targets across host populations. This means that the variability of effectors can result
504 both from their evolution to avoid detection, and from their evolution to maintain their
505 virulence activity (*e.g.*, by targeting one or more potentially polymorphic host proteins to
506 suppress avirulence or basal immunity, or to manipulate other host cellular processes). Our
507 structural modeling suggests in particular that the "coils" and "turns" are the preferred substrate
508 of these coevolutionary interactions leading to the maintenance of elevated polymorphism at
509 MAX virulence effectors. Mirroring the existence of hypervariable MAX effectors, we also detect
510 a substantial proportion of effectors that show no variability, either at the species level or at the
511 lineage level. However, the lack of variability does not necessarily mean they have no impact on
512 virulence. It is possible that their role in virulence is associated with evolutionary constraints
513 that restrict their variability to a limited region of sequence space. Core, monomorphic MAX
514 effectors could be prime targets for genetically-engineered NLRs [57].
515
516 *Expression kinetics of MAX effectors*
517 Expression profiling showed that the MAX effector repertoire was induced specifically and
518 massively during infection. Depending on the host genotype, between 64 and 78% of the MAX
519 effectors were expressed and expression was particularly strong during the early stages of
520 infection. These findings are consistent with previous studies that analyzed genome-wide gene
521 expression during rice infection or specifically addressed MAX effector expression, and they

522 reinforce the hypothesis that MAX effectors are crucial for fungal virulence and specifically
523 involved in the biotrophic phase of infection [17, 38].

524 How this coordinated deployment of the MAX effectors is regulated remains largely
525 unknown. Genome organization does not seem to be a major factor, since MAX effectors do not
526 colocalize and more generally, there is no clustering of effectors in the *P. oryzae* genome, only a
527 slight enrichment in subtelomeric regions [38, 58]. This differs from other pathogenic fungi,
528 such as *Leptosphaeria maculans*, for which early-expressed effectors are clustered in AT-rich
529 isochores, and co-regulated by epigenetic mechanisms [59]. Analysis of promoter regions of
530 MAX effectors did not identify common DNA motifs that may be targeted by transcription
531 factors, and no such transcriptional regulators that would directly regulate large fractions of the
532 effector complement of *P. oryzae* have been identified yet. The few known transcriptional
533 networks controlled by regulators of *P. oryzae* pathogenicity generally comprise different
534 classes of fungal virulence genes, such as secondary metabolism genes or carbohydrate-active
535 enzymes; they are not restricted to effectors. Recently, it was shown that Rgs1, a regulator of G-
536 protein signaling necessary for appressorium development, represses the expression of 60
537 temporally co-regulated effectors in axenic culture and during the pre-penetration stage of plant
538 infection [60]. Of these, six belong to the MAX family and their expression is affected in *cer7* and
539 Δ*rgs1* mutants: MGG_1004T0 [15, 38], MGG_15443T0 [16, 38], MGG_08817T0 [15],
540 MGG_17266T0 [15-17, 38] and MAX15 (MGG_05424T0) and MAX67 (MGG_16175T0), both
541 identified in our study. This represents only 5% of the MAX effectors predicted to date (S2
542 Table) and suggests that multiple complementary mechanisms contribute to the precise
543 coordination of MAX effector expression during rice invasion.

544 Expression profiling also revealed that the plant host genotype strongly influenced the
545 expression of the MAX effector repertoire, suggesting that plasticity in effector expression may
546 contribute to the adaptation of *P. oryzae* to its hosts. MAX effectors were stronger expressed in
547 the more resistant Kitaake rice variety than in highly susceptible Maratelli rice. This is
548 reminiscent of other pathogenic fungi, such as *Fusarium graminearum* and *L. maculans,* for

549 which a relationship between host resistance levels and effector expression was established [61,
550 62]. An expression analysis of MAX effectors in isolates infecting a wider range of host plants
551 with varying resistance levels could be conducted to further investigate the connection between
552 plant resistance and MAX effectors' expression.
553
554 *Presence/absence polymorphism of MAX effectors*
555 Pangenome analyses demonstrated extensive variability in the MAX effector repertoire. In cases
556 where MAX effectors are specifically absent from some lineages, but present in most or all
557 others, it is tempting to hypothesize that they experienced immune-escape loss-of-function
558 mutations that directly contributed to host range expansion or host shifts. A possible example of
559 such a mechanism is the non-MAX effector *PWT3* of *P. oryzae* that is specifically absent from the
560 *Triticum*-infecting lineage [29]. PWT3 triggers resistance in wheat cultivars possessing the
561 *RWT3* resistance gene [63], and its loss was shown to coincide with the widespread deployment
562 of *RWT3* wheat. Similarly, the loss of the effector *AVR1-CO39* (*MAX86*), which is specifically
563 absent from the *Oryza*-infecting lineage and that is detected by the rice NLR immune receptor
564 complex RGA4/RGA5, has been suggested to have contributed to the initial colonization of rice
565 by the *Setaria*-infecting lineage [20, 31, 64]. Two other orthologous *P. oryzae* effectors, *PWL1*
566 and *PWL2*, exclude Eleusine and rice-associated isolates from infecting *Eragrostis curvula*, and
567 can, therefore, also be considered as host-specificity determinants [28, 65]. Interestingly,
568 ALPHAFOLD predicts PWL2 to adopt a MAX effector fold [66]. In our study, however, gene knock-
569 in experiments with *MAX79*, *MAX83,* and *MAX89* - specifically absent from the *Oryza*-infecting
570 lineage - did not reveal a strong effect on virulence towards a large panel of rice varieties. Hence,
571 unlike AVR1-CO39, these effectors are not key determinants of host-specificity. This suggests
572 that overcoming non-host resistance is not the only and maybe not the main evolutionary
573 scenario behind the specific loss of MAX effectors in the *Oryza*-infecting lineage. A possible
574 alternative mechanism that can explain massive MAX effector loss during host shifts is a lack of
575 functionality in the novel host. Some MAX effectors from a given lineage may have no function in

576 the novel host, simply because their molecular targets are absent or too divergent in the novel
577 host. Cellular targets of fungal effectors remain unknown for the most part, but knowledge of the
578 molecular interactors of MAX effectors may help shed light on the drivers of their
579 presence/absence polymorphism.
580
581 *Concluding remarks*
582 The discovery of large, structurally-similar, effector families in pathogenic fungi and the
583 increasing availability of high-quality whole genome assemblies and high-confidence annotation
584 tools, pave the way for in-depth investigations of the evolution of fungal effectors by
585 interdisciplinary approaches combining state-of-the-art population genomics, protein structure
586 analysis, and functional approaches. Our study on MAX effectors in the model fungus and
587 infamous cereal killer *P. oryzae* demonstrates the power of such an approach. Our investigations
588 reveal the fundamental role of directional and balancing selection in shaping the diversity of
589 MAX effector genes and pinpoint specific positions in the proteins that are targeted by these
590 evolutionary forces. This type of knowledge is still very limited on plant pathogens, and there
591 are very few studies compared to the plethoric literature on the evolution of virulence factors in
592 human pathogens. Moreover, by revealing the concerted and plastic deployment of the MAX
593 effector repertoire, our study highlights the current lack of knowledge on the regulation of these
594 processes. A major challenge will now be to identify the regulators, target proteins and mode of
595 action of MAX effectors, in order to achieve a detailed understanding of the relationships
596 between the structure, function and evolution of these proteins.

METHODS

Genome assemblies, gene prediction, and pan-genome analyses

Among the 120 genome assemblies included in our study, 66 were already assembled and publicly available, and 54 were newly assembled (S1 Table). For the 54 newly assembled genomes, reads were publicly available for 50 isolates, and four additional isolates were sequenced (available under BioProject PRJEB47684). For the four sequenced isolates, DNA was extracted using the same protocol as in ref. [67]. TruSeq nano kits were used to prepare DNA libraries with insert size of ~500bp for 150 nucleotide paired-end indexed sequencing with Illumina HiSeq 3000. For the 54 newly generated assemblies, CUTADAPT [68] was used for trimming and removing low-quality reads, reads were assembled with ABYSS 1.9.0 [69] using eight different K-mer sizes, and we chose the assembly produced with the K-mer size that yielded the largest N50. For all 120 genome assemblies, genes were predicted by BRAKER 1 [70] using RNAseq data from ref. [21] and protein sequences of isolate 70-15 (Ensembl Fungi release 43). To complement predictions from BRAKER, we also predicted genes using AUGUSTUS 3.4.0 [56] with RNAseq data from ref. [21] , protein sequences of isolate 70-15 (Ensembl Fungi release 43), and *Magnaporthe grisea* as the training set. Gene predictions from BRAKER and AUGUSTUS were merged by removing the genes predicted by AUGUSTUS that overlapped with genes predicted by BRAKER. Repeated elements were masked with REPEATMASKER 4.1.0 (http://www.repeatmasker.org/). The quality of genome assembly and gene prediction was checked using BUSCO 4.0.4 [32]. The homology relationships among predicted genes were identified using ORTHOFINDER v2.4.0 [36]. The size of pan- and core-genomes was estimated using rarefaction, by resampling combinations of one to 119 genomes, taking a maximum of 100 resamples by pseudo-sample size. Sequences for each orthogroup were aligned at the codon level (i.e., keeping sequences in coding reading frame) with TRANSLATORX 1.1 [71], using MAFFT v7 [72] as the aligner and default parameters for GBLOCKS 0.91B [73]. The effect of assembly properties, host of origin, and study of origin on the number of predicted genes computed from

the orthology table was analyzed in PYTHON 3.7 using the function in PEARSONR in SCIPY.STATS 1.10.1, and functions FORMULA.API.OLS and STATS.ANOVA.ANOVA_LM in STATSMODELS 0.15.0.

Identification of effectors sensu lato, and MAX effectors

We predicted the secretome by running SIGNALP 4.1 [74], TARGETP 1.1 [75], and PHOBIUS 1.01 [62] to identify signal peptides in the translated coding sequences of 12000 orthogroups. Only proteins predicted to be secreted by at least two methods were retained. Transmembrane domains were identified using TMHMM [76] and proteins with a transmembrane domain outside the 30 first amino acids were excluded from the predicted secretome. Endoplasmic reticulum proteins were identified with PS-SCAN (https://ftp.expasy.org/databases/prosite/ps_scan/), and excluded.

To identify MAX effectors, we used the same approach as in the original study that described MAX effectors [17]. We first used PSI-BLAST 2.6.0 [33] to search for homologs of known MAX effectors (AVR1-CO39, AVR-Pia, AvrPiz-t, AVR-PikD, and ToxB) in the predicted secretome. Significant PSI-BLAST hits (e-value < e-4) were aligned using a structural alignment procedure implemented in TM-ALIGN [35]. Three rounds of HMMER [34] searches were then carried out, each round consisting of alignment using TM-ALIGN version 20140601, model building using HMMBUILD, and HMM search using HMMSEARCH (e-value < e-3). Only proteins with two expected conserved cysteines less than 33-48 amino acids apart were retained in the first two rounds of HMMER searches, as described in ref. [17].

Subsequent evolutionary analyses were conducted on three sets of orthogroups: MAX effectors, putative effectors, and other genes. The “MAX” group corresponded to 80 orthogroups for which at least 10% of sequences were identified as MAX effectors. The “secreted proteins” groups corresponded to 3283 orthogroups that were not included in the MAX group, and for which at least 10% of sequences were predicted to be secreted proteins. The last group included the remaining 11404 orthogroups.

651 For missing MAX effector sequences, we conducted an additional similarity search to
652 correct for gene prediction errors. For a given MAX orthogroup and a given isolate, if a MAX
653 effector was missing, we used BLAST-N to search for significant hits using the longest sequence of
654 the orthogroup as the query sequence, and the isolate's genome assembly as the subject
655 sequence (S3 Table). We also corrected annotation errors, such as the presence of very short
656 (typically <50bp) or very long (typically >500bp) introns, missing terminal exons associated
657 with premature stops, or frameshifts caused by indels. All these annotation errors were checked,
658 and corrected manually if needed, using the RNAseq data used in gene prediction in the
659 INTEGRATIVE GENOME VIEWER [77, 78]. We also found that some orthogroups included chimeric
660 genes resulting from the erroneous merging of two genes that were adjacent in assemblies. This
661 was the case for orthogroups OG0000093 and OG0010985, and we used RNA-seq data in the
662 INTEGRATIVE GENOME VIEWER to split the merged genic sequences and keep only the sequence
663 corresponding to a MAX effector.

664 For evolutionary analyses conducted on single-copy orthologs, the 11 orthogroups that
665 included paralogous copies of MAX effectors were split into sets of orthologous sequences using
666 genealogies inferred using RAXML v8 [37], yielding a total of 94 single-copy MAX orthologs, of
667 which 90 orthologs passed our filters on length and sample size to be included in evolutionary
668 analyses (see below). For each split orthogroup, sets of orthologous sequences were assigned a
669 number that was added to the orthogroup's identifier as a suffix (for instance paralogous
670 sequences of orthogroup OG0000244 were split into orthogroups OG0000244_1 and
671 OG0000244_2). Sequences were re-aligned using TRANSLATORX (see above) after splitting
672 orthogroups.

673 All genome assemblies, gene models, aligned coding sequences for all orthogroups, and
674 single-copy orthologs, are available in Zenodo, doi: 10.5281/zenodo.7689273 and doi:
675 10.5281/zenodo.8052494.

676

677 *Analysis of population subdivision*

678 Population structure was inferred from SNPs identified in GBLOCKS-cleaned alignments of coding
679 sequences at 7317 single-copy core orthologs (described in section *Genome assemblies, gene*
680 *prediction, and pan-genome analyses*). We kept only one randomly chosen four-fold degenerate
681 synonymous site per single-copy core ortholog. We used the sNMF method from the LEA
682 package in R [40] to infer individual ancestry coefficients in *K* ancestral populations. We used
683 SPLITSTREE version 5.3 [41] to visualize relationships between genotypes in a phylogenetic
684 network, with reticulations to represent the conflicting phylogenetic signals caused by
685 homoplasy.
686
687 *Homology modeling of MAX effectors*
688 To check that orthogroups predicted to be MAX effectors had the typical 3D structure of MAX
689 effectors with two beta sheets of three beta strands each, eight experimental structures with
690 MAX-like folds were selected as 3D templates for homology modeling (PDB identifiers of the
691 templates: 6R5J, 2MM0, 2MM2, 2MYW, 2LW6, 5A6W, 5Z1V, 5ZNG). For each of the 94 MAX
692 orthologous groups, one representative protein was selected and homology models of this 1D
693 query relative to each 3D template were built using MODELLER [79] with many alternative query-
694 template threading alignments. The structural models generated using the alternative
695 alignments were evaluated using a combination of six structural scores (DFIRE [80], GOAP [81],
696 and QMEAN's E_{1D}, E_{2D}, E_{3D} scores [82]). A detailed description of the homology modeling
697 procedure is provided in S2 Text. The best structural models for the 94 representative
698 sequences of each group of MAX orthologs are available
699 at https://pat.cbs.cnrs.fr/magmax/model/. The correspondence between MAX orthogroups
700 identifiers used in homology modeling and MAX orthogroups identifiers resulting from gene
701 prediction is given in S2 Table. Protein models were visualized with PYMOL 2.5 [83].
702
703 *Evolutionary analyses*

704 Lineage-level analyses were conducted on a dataset from which divergent or introgressed
705 isolates were removed (G17 from *Eragrostis*, Bm88324 & Bd8401 from *Setaria*, 87-120; BF0072
706 and BN0019 from *Oryza*; IR0088 from *Echinochloa*), to limit the impact of population
707 subdivision within lineages. The *Stenotaphrum*-infecting lineage was not included in lineage-
708 level analyses due to the small sample size.

709 Nucleotide diversity [84], synonymous and non-synonymous nucleotide diversity, and
710 population differentiation [45] were estimated using EGGLIB v3 [85] using classes COMPUTESTATS
711 and CODINGDIVERSITY. Sites with more than 30% missing data were excluded. Orthogroups with
712 less than 10 sequences (*nseff*<10, *nseff* being the average number of used samples among sites
713 that passed the missing data filter) or shorter than 30bp (*lseff*<30, *lseff* being the number of sites
714 used for analysis after filtering out sites with too many missing data) were excluded from
715 computations. For analyses of polymorphism at secondary structure annotations, the cutoff on
716 *lseff* was set at 10bp.

717 For the computation of d_N/d_S and quantification of adaptive evolution, we used isolate
718 NI919 of *Pyricularia* sp. LS [47, 48] as the outgroup (assembly GCA_004337975.1, European
719 Nucleotide Archive). Genes were predicted in the outgroup assembly using EXONERATE v2.2
720 CODING2GENOME [86]. For each gene, the query sequence was a *P. oryzae* sequence randomly
721 selected among sequences with the fewest missing data. In parsing EXONERATE output, we
722 selected the sequence with the highest score, with a length greater than half the length of the
723 query sequence.

724 The d_N/d_S ratio was estimated using a maximum likelihood approach (runmode=-2,
725 CodonFreq=2 in CODEML [87]), in pairwise comparisons of protein coding sequences (*i.e.*,
726 without using a phylogeny). For each d_N/d_S we randomly selected 12 ingroup sequences and
727 computed the average d_N/d_S across the 12 ingroup/outgroup pairs.

728 Kruskal-Wallis tests were performed using the SCIPY.STATS.KRUSKAL library in PYTHON 3.7.
729 Posthoc Mann-Whitney U-tests were performed using the SCIKIT_POSTHOCS library in PYTHON 3.7,
730 with p-values adjusted using the Bonferroni-Holm method.

731 Amino acid change data was modeled using a binomial generalized linear mixed model
732 with function GLMER with package LME4 version 1.1-32 in R version 4.1.2. Interactions between
733 predictor variables were not significant and thus not included in the model presented in the
734 Results section.
735
736 *Constructs for the transformation of fungal isolates*
737 PCR products used for cloning were generated using the Phusion High-Fidelity DNA Polymerase
738 (Thermo Fisher) and the primers listed in S7 Table. Details of the constructs are given in S8
739 Table. Briefly, the pSC642 plasmid (derived from the pCB1004 vector), containing a cassette for
740 the expression of a gene of interest under the control of the *AVR-Pia* promoter (*pAVR-Pia*) and
741 the *Neurospora crassa β-tubulin* terminator (*t-tub*), was amplified by PCR with primers oML001
742 and oTK609 for the insertion of MAX genes listed in S9 Table. The MAX genes
743 *Mo_US0071_000070* (*MAX79*), *Mo_US0071_046730* (*MAX89*) and *Mo_US0071_115900*
744 (*MAX83*), amplified by PCR from genomic DNA of the *P. oryzae* isolate US0071, were inserted
745 into this vector using the Gibson Assembly Cloning Kit (New England BioLabs). The final
746 constructs were linearized using the KpnI restriction enzyme (Promega) before *P. oryzae*
747 transformation.
748
749 *Plant and fungal growth conditions*
750 Rice plants (*Oryza sativa*) were grown in a glasshouse in a substrate of 31% coconut peat, 30%
751 Baltic blond peat, 15% Baltic black peat, 10% perlite, 9% volcanic sand, and 5% clay,
752 supplemented with 3.5 $g.L^{-1}$ of fertilizer (Basacote High K 6M, NPK 13-5-18). Plants were grown
753 under a 12h-light photoperiod with a day-time temperature of 27 °C, night-time temperature of
754 21 °C, and 70% humidity. For spore production, the wild-type and transgenic isolates of *P.*
755 *oryzae* Guy11 were grown for 14 days at 25°C under a 12h-light photoperiod on rice flour agar
756 medium (20 $g.L^{-1}$ rice seed flour, 2.5 $g.L^{-1}$ yeast extract, 1.5% agar, 500.000U penicillin g),
757 supplemented with 240 $\mu g.ml^{-1}$ hygromycin for transgenic isolates. For mycelium production,

758 plugs of mycelium of *P. oryzae* Guy11 were grown in liquid medium (10 g.L^{-1} glucose, 3 g.L^{-1}
759 KNO_3, 2 g.L^{-1} KH_2PO_4, 2,5 g.L^{-1} yeast extract, 500 000U penicillin g) for 5 days at 25°C in the
760 dark under agitation.
761
762 *Fungal transformation*
763 Protoplasts from the isolate Guy11 of *P. oryzae* were transformed by heat shock with 10µg of
764 KpnI-linearized plasmids for the expression of MAX effectors or RFP as described previously
765 [88]. After two rounds of antibiotic selection and isolation of monospores, transformed isolates
766 were genotyped by Phire Plant Direct PCR (Thermo Scientific) using primers described in S7
767 Table. The Guy11 transgenic isolates expressing *AVR-Pia* and *AVR1-CO39* were previously
768 generated [50, 89].
769
770 *Fungal growth and infection assays*
771 For the analysis of interaction phenotypes, leaves of three-week-old rice plants were spray-
772 inoculated with conidial suspensions (40 000 conidia.ml^{-1} in water with 0.5% gelatin). Plants
773 were incubated for 16 hours in the dark at 25°C and 95% relative humidity, and then grown for
774 six days in regular growth conditions. Seven days after inoculation, the youngest leaf that was
775 fully expanded at the time of inoculation was collected and scanned (Scanner Epson Perfection
776 V370) for further symptoms analyses. Phenotypes were qualitatively classified according to
777 lesion types: no lesion or small brown spots (resistance), small lesions with a pronounced
778 brown border and a small gray center (partial resistance), and larger lesions with a large gray
779 center or dried leaves (susceptibility). For the analysis of gene expression, plants were spray-
780 inoculated with conidial suspensions at 50 000 conidia.ml^{-1} (in water with 0.5% gelatin), and
781 leaves were collected three days after inoculation.
782
783 *RNA extraction and qRT-PCR analysis*

784 Total RNA extraction from rice leaves or Guy11 mycelium and reverse transcription were
785 performed as described by ref. [90]. Briefly, frozen leaves and mycelium were mechanically
786 ground. RNA was extracted using TRI-reagent (Sigma-Aldrich) and chloroform separation.
787 Denaturated RNA (5µg) was retrotranscribed and used for quantitative PCR using GoTaq qPCR
788 Master Mix according to the manufacturer's instructions (Promega) at a dilution of 1/10 for
789 mycelium and 1/7 for rice leaves. The primers used are described in S7 Table. Amplification was
790 performed as described by ref. [90] using a LightCycler480 instrument (Roche), and data were
791 extracted using the instrument software. To calculate *MAX* gene expressions, the $2^{-\Delta\Delta CT}$ method
792 and primers measured efficiency were used. Gene expression levels are expressed relative to the
793 expression of constitutive reference gene *MoEF1α*.
794
795 *Statistical analyses of phenotypic data*
796 For expression comparison between Kitaake and Maratelli infection, all analyses were
797 performed using R (www.r-project.org). The entire kinetic experiment was repeated three times
798 with five biological replicates for each time point. For each variety, gene, and experimental
799 replicate, values corresponding to the day post-inoculation with the highest median expression
800 were extracted for statistical analyses. Expression data were not normally distributed so for
801 each gene, differences between varieties were evaluated using non-parametric Mann-Whitney
802 U-tests.
803
804 **SUPPORTING INFORMATION**
805 S1 Table. Genomic assemblies with metadata.
806 S2 Table. Nomenclature of MAX effectors predicted in this study and in previous reports.
807 S3 Table. Presence/absence of MAX effector orthologs.
808 S4 Table. The expression of *MAX79*, *MAX83* and *MAX89* in Guy11 does not trigger recognition in a panel of
809 rice varieties.
810 S5 Table. Gene average of summary statistics of polymorphism, differentiation and divergence.

S6 Table. π_N and d_N/d_S in different classes of secondary structure annotations for MAX effectors with $\pi_N/\pi_S>1$ and $d_N/d_S>1$, respectively.

S7 Table. Primers for cloning and expression analyses.

S8 Table. Vector constructs.

S9 Table. Sequences of the MAX effectors in the isolate US0071 that were used for the complementation of Guy11.

S1 Figure. Effect of assembly properties on the number of genes.

S2 Figure. Expression patterns of MAX effectors during rice infection.

S3 Figure. Differential expression levels of MAX effectors upon infection of two different rice cultivars.

S4 Figure. Nucleotide diversity (π), ratio of non-synonymous to synonymous nucleotide diversity (π_N/π_S), orthogroup frequency for MAX effectors, other secreted proteins, and other genes.

S5 Figure. Frequency of MAX effector orthogroups as a function of the frequency of the adjacent orthogroups in the genome.

S6 Figure. Analyses of population subdivision with sNMF.

S7 Figure. *MAX79*, *MAX83* and *MAX89* are expressed in the transgenic Guy11 isolates upon rice inoculation.

S8 Figure. F_{ST} versus π_N/π_S at MAX effectors

S9 Figure. Amino acid changes segregating in *P. oryzae* at MAX effectors with an avirulence function and MoToxB (first row), and MAX effectors with $\pi_N/\pi_S>2$ (next rows); amino acid changes are shown in dark blue and known binding interfaces in light blue. Note that the π_N/π_S ratio is >2 for the avirulence genes *AvrPiz-t* and AVR-Pik. Proteins are displayed twice, with one copy rotated 180 degrees around a vertical axis. The interface involved in binding with host proteins is known for AVR1-CO39, AVR-Pia, and AVR-Pik only ([50-53]).

S10 Figure. Secondary structure annotations of MAX effectors aligned with TM-ALIGN.

S1 Data. Summary statistics per orthogroup.

S2 Data. Summary statistics per MAX effector ortholog, species wide, and per lineage.

S3 Data. Structural properties and polymorphism of amino acids in MAX effectors.

841 S1 Text. Fitting a generalized linear model to amino acid polymorphism data.

842 S2 Text. Homology modeling procedure.

843 **FIGURES AND TABLES**

844 Figure 1. Schematic representation of the main steps of the bioinformatic pipeline used to
845 predict genes in 120 genomes of *Pyricularia oryzae*, to identify genes encoding MAX effectors,
846 and to measure their genetic variability. References: Gladieux et al. 2018 [27]; Pordel et al. 2021
847 [21]. Genome assembly and annotation: using RNAseq and reference proteins, we predicted
848 genes with AUGUSTUS 3.4.0 [56] and BRAKER 1 [70] in 54 genomes that were assembled in this
849 study with ABYSS 1.9.0 [69], as well as in 66 assemblies that were published earlier; repeated
850 sequences were masked using REPEATMASKER 4.1.0 (http://www.repeatmasker.org/). Secretome
851 prediction: we identify signal peptides in the predicted genes by running SIGNALP 4.1 [74],
852 TARGETP 1.1 [75], and PHOBIUS 1.01 [62], removing genes encoding proteins with a predicted
853 transmembrane domain (identified using TMHMM [76]), as well as endoplasmic reticulum
854 proteins (identified with PS-SCAN from expasy.org). Prediction of MAX effectors: MAX effectors
855 were identified using PSI-BLAST [33] to search for homologs of known MAX effectors (AVR1-
856 CO39, AVR-Pia, AvrPiz-t, AVR-PikD, and ToxB) in the predicted secretome, followed by
857 structure-guided alignment of PSI-BLAST hits using TM-ALIGN [35], and three iterative rounds of
858 HMMER [34] searches based on HMMBUILD models built on TM-ALIGN alignments of significant
859 hits. Only proteins with two expected conserved cysteines less than 33-48 amino acids apart
860 were retained [17]. Evolutionary analyses: the 11 orthogroups that included paralogous copies
861 of MAX effectors were split into sets of orthologous sequences using genealogies inferred using
862 RAXML v8 [37], yielding a total of 94 single-copy MAX orthologs for evolutionary analyses;
863 protein structure models were inferred using homology modeling in MODELLER [79], and
864 structural features were identified with STRIDE [91].

865

866 Figure 2. The expression of *MAX* genes is biotrophy-specific and is influenced by the host plant.
867 (A) Transcript levels of *MAX* genes and the biotrophy marker gene *Bas3* were determined by

868 qRT-PCR in the mycelium (Myc) of the *P. oryzae* isolate Guy11 grown for 5 days in liquid culture,
869 and in infected leaves of the rice cultivars Maratelli and Kitaake at 2, 3, 4, and 7 days post
870 inoculation (dpi) with Guy11. Relative expression levels were calculated using the constitutively
871 expressed *MoEF1α* (*Elongation Factor 1α*) gene as a reference. The heatmap shows the median
872 relative expression value for each gene (in log2 scale), calculated from 6 independent biological
873 samples for the Myc condition, and 3 independent inoculation experiments (each with 5
874 independent leaf samples per time point) for each rice cultivar. Effectors were ranked from top
875 to bottom by increasing relative expression values in Maratelli. Relative expression values were
876 assigned to six categories: not expressed (<0.008), very weakly (0.008-0.04), weakly (0.04-0.2),
877 moderately (0.2-1), strongly (1-5) and very strongly expressed (>5). (B) Scatter plot comparing
878 the relative expression levels of *MAX* genes in Guy11-infected Maratelli and Kitaake cultivars.
879 Each point shows the maximum median relative expression value (in log10 scale) calculated in
880 the infection kinetics described in (A). Difference in effector relative expression levels between
881 the two conditions was assessed by Mann-Whitney U tests and dots were colored according to
882 significance results: grey ($p>0.05$), yellow ($p<0.05$), orange ($p<0.001$), red ($p<0.0001$), black
883 (effectors not expressed in both conditions).
884
885 Figure 3. The pan-genome of *P. oryzae*. (A) Composition of the pangenome of MAX effectors,
886 other secreted proteins, and other genes. (B) Rarefaction analysis of the size of pan- and core-
887 genomes. For k ranging from two to the sample size minus one, pan- and core-genome sizes
888 were computed for 1000 random combinations of k isolates. Subsample size is represented as a
889 fraction of the sample size (n=120), and pan- and core-genome sizes as a fraction of maximum
890 gene counts (reported at the center of donut plots in panel A). "core" genes are present in all
891 isolates of a pseudo-sample of size k; "pan" qualifies genes that are not "core". (C) Nucleotide
892 diversity per base pair (π) in core, softcore, and shell genes. A number of data points were
893 cropped from the nucleotide diversity plot for visually optimal presentation but included in
894 statistical tests. In box plots, the black circle is the mean, the black line is the median. Cloud

895 genes were not included in the nucleotide diversity plot because it was not computable due to
896 the small sample size or lack of sequence after filtering for missing data. Shared superscripts
897 indicate non-significant differences (Post-hoc Mann-Whitney U-tests).
898
899 Figure 4. Population subdivision in 120 isolates of *Pyricularia oryzae*. Population subdivision
900 was inferred from (A-B) 6780 polymorphisms at four-fold degenerate synonymous sites
901 identified in coding sequences of single-copy core orthologs (one polymorphism without
902 missing data randomly chosen per ortholog), (C) 130 SNPs without missing data identified in
903 coding sequences of single-copy core MAX effectors, and (D) a table of presence/absence data
904 (coded as 0 and 1) for all 80 MAX effector orthogroups. (A) Genetic ancestry proportions for
905 individual isolates in K=8 ancestral populations, as estimated using the sNMF clustering
906 algorithm [40]; each isolate is depicted as a horizontal bar divided into K segments representing
907 the proportion of ancestry in K=8 inferred ancestral populations; host genus of origin is
908 indicated on the right side. (B-D) Neighbor-net phylogenetic networks estimated with
909 SplitsTree [41], with isolate names colored according to their host of origin.
910
911 Figure 5. AVR1-CO39 contributes to non-host specificity in rice but not MAX79, MAX83 or
912 MAX89. Wild type and transgenic isolates of *P. oryzae* Guy11 expressing the *RFP* (*red*
913 *fluorescent protein*), *AVR-Pia, AVR1-CO39, MAX79*, *MAX83* or *MAX89* gene were spray-
914 inoculated at 40 000 spores/ml on three-week-old rice plants of the cultivars Aichi Asahi (A)
915 and Nipponbare (B). For each condition, representative disease phenotypes on rice leaves at
916 seven days post-inoculation are shown (top panels, R: resistance, S: susceptibility). Disease
917 phenotypes were also scored (from 1 [complete resistance] to 6 [high susceptibility]) on leaves
918 from three to five individual rice plants and data are shown as dot plots (bottom panels). The
919 size of each circle is proportional to the number of replicates (n) matching the corresponding
920 score for each condition. Small red dots correspond to individual measurements. The
921 experiment was performed twice for Aichi Asahi and four times for Nipponbare for all isolates

922 except for WT, AVR-Pia, and AVR1-CO39 control isolates. For these isolates, experiments were
923 performed once on Aichi Asahi and twice on Nipponbare because disease phenotypes are well
924 characterized in the literature.
925
926 Figure 6. Summary statistics of polymorphism and divergence at MAX effectors, other secreted
927 proteins (i.e., secretome), and other genes of *P. oryzae*. (A) Species-wide estimates of π
928 (nucleotide diversity per bp), F_{ST} (the amount of differentiation among lineages), π_N (non-
929 synonymous nucleotide diversity per bp), π_S (synonymous nucleotide diversity per bp), π_N/π_S
930 (the ratio of non-synonymous to synonymous nucleotide diversity), d_N/d_S (the ratio of non-
931 synonymous to synonymous rates of substitutions). (B) Lineage-specific estimates of π_N/π_S. (C)
932 Amino acid changes segregating in *P. oryzae* at MAX effectors with an avirulence function and
933 MoToxB (first row) and MAX effectors with $\pi_N/\pi_S>2$ (next rows); amino acid changes are shown
934 in dark blue and known binding interfaces in light blue; all effectors are represented with the
935 same orientation as AvrPiz-t in panel (B). Note that the π_N/π_S ratio is >2 for the avirulence
936 genes *AvrPiz-t* and AVR-Pik. Proteins are displayed twice in panels C and E, with one copy
937 rotated 180 degrees around a vertical axis. The interface involved in binding with host proteins
938 is known for AVR1-CO39, AVR-Pia, and AVR-Pik only ([50-53]). (D) and (E) Species-wide
939 estimates of π_N and d_N/d_S computed at MAX effectors with signatures of balancing selection
940 ($\pi_N/\pi_S>1$; panel D) and signatures of directional selection ($d_N/d_S>1$; panel E) for different
941 classes of structural features highlighted on the three-dimensional structure of *AvrPiz-t* above
942 panel D: (i) secondary structure elements, with three subclasses: "coils", "extended
943 conformation", and "turns"; (ii) solvent accessibility percentage of the Van der Waals surface of
944 the amino acid side chain, with three sub-classes: 0-30% (buried), 30-60% (intermediate), and
945 60-100% (exposed); (iii) structural domains, with six subclasses that grouped the coil, extended
946 conformation and turn residues that define the six beta strands characteristic of MAX effectors.
947 In the heatmaps, each line represents a MAX effector. For a given MAX effector and a given
948 structural feature, the darkest color indicates the class of the structural feature for which the

summary statistic is the highest. Only single-copy core, softcore, and shell groups of orthologous genes were included in the calculations. Shared superscripts indicate non-significant differences (post-hoc Mann-Whitney U-tests, $p>0.05$). A number of data points were cropped from plots in (A) and (B) for visually optimal presentation but included in statistical tests. In box plots, the black circle is the mean, the black line is the median.

REFERENCES

1. Schulze-Lefert P, Panstruga R. A molecular evolutionary concept connecting nonhost resistance, pathogen host range, and pathogen speciation. Trends in Plant Science. 2011;16(3):117-25. doi: 10.1016/j.tplants.2011.01.001.
2. Sánchez-Vallet A, Fouché S, Fudal I, Hartmann FE, Soyer JL, Tellier A, et al. The genome biology of effector gene evolution in filamentous plant pathogens. Annual review of phytopathology. 2018;56:21-40.
3. Haldane JBS. Disease and evolution. Ricerca Scient 1949;19:68-76.
4. Flor HH. Inheritance of pathogenicity in Melampsora lini. Phytopathology. 1942;32:653-69.
5. Barrett JA. Frequency-dependent selection in plant-fungal interactions. Philosophical Transactions of the Royal Society of London B, Biological Sciences. 1988;319(1196):473-83.
6. Bergelson J, Kreitman M, Stahl EA, Tian D. Evolutionary dynamics of plant R-genes. Science. 2001;292(5525):2281-5.
7. Brown JKM. Chance and selection in the evolution of barley mildew. Trends in Microbiology. 1994;2(12):470-5. PubMed PMID: 29.
8. Brown JKM. Durable resistance of crops to disease: a Darwinian perspective. Annual review of phytopathology. 2015;53:513-39.
9. Stahl EA, Dwyer G, Mauricio R, Kreitman M, Bergelson J. Dynamics of disease resistance polymorphism at the Rpm1 locus of Arabidopsis. Nature. 1999;400(6745):667-71.
10. Gladieux P, van Oosterhout C, Fairhead S, Jouet A, Ortiz D, Ravel S, et al. Extensive immune receptor repertoire diversity in disease-resistant rice landraces. bioRxiv. 2022:2022-12.
11. Bakker EG, Toomajian C, Kreitman M, Bergelson J. A genome-wide survey of R gene polymorphisms in Arabidopsis. The Plant cell. 2006;18(8):1803-18.
12. Bakker EG, Traw MB, Toomajian C, Kreitman M, Bergelson J. Low levels of polymorphism in genes that control the activation of defense response in Arabidopsis thaliana. Genetics. 2008;178(4):2031-43.
13. Ebert D, Fields PD. Host–parasite co-evolution and its genomic signature. Nature Reviews Genetics. 2020;21(12):754-68.
14. Ebbole DJ, Chen M, Zhong Z, Farmer N, Zheng W, Han Y, et al. Evolution and Regulation of a Large Effector Family of Pyricularia oryzae. Molecular Plant-Microbe Interactions. 2021;34(3):255-69.
15. Seong K, Krasileva KV. Computational structural genomics unravels common folds and novel families in the secretome of fungal phytopathogen Magnaporthe oryzae. Molecular Plant-Microbe Interactions. 2021;34(11):1267-80.
16. Seong K, Krasileva KV. Prediction of effector protein structures from fungal phytopathogens enables evolutionary analyses. Nature Microbiology. 2023;8(1):174-87.
17. de Guillen K, Ortiz-Vallejo D, Gracy J, Fournier E, Kroj T, Padilla A. Structure analysis uncovers a highly diverse but structurally conserved effector family in phytopathogenic fungi. PLoS Pathog. 2015;11(10):e1005228.
18. Savary S, Willocquet L, Pethybridge SJ, Esker P, McRoberts N, Nelson A. The global burden of pathogens and pests on major food crops. Nature ecology & evolution. 2019;3(3):430.
19. Fernandez J, Orth K. Rise of a cereal killer: the biology of Magnaporthe oryzae biotrophic growth. Trends in microbiology. 2018;26(7):582-97.
20. Couch BC, Fudal I, Lebrun M-H, Tharreau D, Valent B, van Kim P, et al. Origins of Host-Specific Populations of the Blast Pathogen *Magnaporthe oryzae* in Crop Domestication With Subsequent Expansion of Pandemic Clones on Rice and Weeds of Rice. Genetics. 2005;170(2):613-30. PubMed PMID: 61.
21. Pordel A, Ravel S, Charriat F, Gladieux P, Cros-Arteil S, Milazzo J, et al. Tracing the origin and evolutionary history of Pyricularia oryzae infecting maize and barnyard grass. Phytopathology. 2021;111(1):128-36.
22. Kato H, Yamamoto M, Yamaguchi-Ozaki T, Kadouchi H, Iwamoto Y, Nakayashiki H, et al. Pathogenicity, mating ability and DNA restriction fragment length polymorphisms of Pyricularia populations isolated from Gramineae, Bambusideae and Zingiberaceae plants. Journal of General Plant Pathology. 2000;66:30-47.
23. Urashima AS, Igarashi S, Kato H. Host range, mating type, and fertility of Pyricularia grisea from wheat in Brazil. Plant Disease. 1993;77(12):1211-6.
24. Igarashi S. Pyricularia em trigo. 1. Ocorrencia de Pyricularia sp noestado do Parana. Fitopatol Bras. 1986;11:351-2.
25. Milazzo J, Pordel A, Ravel S, Tharreau D. First scientific report of Pyricularia oryzae causing gray leaf spot disease on perennial ryegrass (Lolium perenne) in France. Plant Disease. 2019;103(5):1024-.

26. Islam MT, Croll D, Gladieux P, Soanes DM, Persoons A, Bhattacharjee P, et al. Emergence of wheat blast in Bangladesh was caused by a South American lineage of Magnaporthe oryzae. BMC biology. 2016;14(1):84.
27. Gladieux P, Condon B, Ravel S, Soanes D, Maciel JLN, Nhani A, et al. Gene Flow between Divergent Cereal- and Grass-Specific Lineages of the Rice Blast Fungus Magnaporthe oryzae. mBio. 2018;9(1).
28. Sweigard JA, Carroll AM, Kang S, Farrall L, Chumley FG, Valent B. Identification, Cloning, and Characterization of *PWL2*, a Gene for Host Species Specificity in the Rice Blast Fungus. The Plant cell. 1995;7(8):1221-33. PubMed PMID: 260.
29. Inoue Y, Vy TTP, Yoshida K, Asano H, Mitsuoka C, Asuke S, et al. Evolution of the wheat blast fungus through functional losses in a host specificity determinant. Science. 2017;357(6346):80-3.
30. Asuke S, Tanaka M, Hyon G-S, Inoue Y, Vy TTP, Niwamoto D, et al. Evolution of an Eleusine-specific subgroup of Pyricularia oryzae through a gain of an avirulence gene. Molecular Plant-Microbe Interactions. 2020;33(2):153-65.
31. Zheng Y, Zheng W, Lin F, Zhang Y, Yi Y, Wang B, et al. AVR1-CO39 is a predominant locus governing the broad avirulence of Magnaporthe oryzae 2539 on cultivated rice (Oryza sativa L.). Molecular plant-microbe interactions. 2011;24(1):13-7.
32. Simão FA, Waterhouse RM, Ioannidis P, Kriventseva EV, Zdobnov EM. BUSCO: assessing genome assembly and annotation completeness with single-copy orthologs. Bioinformatics. 2015;31(19):3210-2.
33. Altschul SF, Madden TL, Schäffer AA, Zhang J, Zhang Z, Miller W, et al. Gapped BLAST and PSI-BLAST: a new generation of protein database search programs. Nucleic acids research. 1997;25(17):3389-402.
34. Finn RD, Clements J, Eddy SR. HMMER web server: interactive sequence similarity searching. Nucleic acids research. 2011;39(suppl_2):29-37.
35. Zhang Y, Skolnick J. TM-align: a protein structure alignment algorithm based on the TM-score. Nucleic acids research. 2005;33(7):2302-9.
36. Emms DM, Kelly S. OrthoFinder: solving fundamental biases in whole genome comparisons dramatically improves orthogroup inference accuracy. Genome biology. 2015;16(1):157.
37. Stamatakis A. RAxML version 8: a tool for phylogenetic analysis and post-analysis of large phylogenies. Bioinformatics. 2014;30(9):1312-3.
38. Yan X, Tang B, Ryder LS, MacLean D, Were VM, Eseola AB, et al. The transcriptional landscape of plant infection by the rice blast fungus Magnaporthe oryzae reveals distinct families of temporally co-regulated and structurally conserved effectors. The Plant cell. 2023;35(5):1360-85.
39. Fay JC, Wu C-I. Sequence divergence, functional constraint, and selection in protein evolution. Annual review of genomics and human genetics. 2003;4(1):213-35.
40. Frichot E, Mathieu F, Trouillon T, Bouchard G, François O. Fast and efficient estimation of individual ancestry coefficients. Genetics. 2014;196(4):973-83.
41. Huson DH, Bryant D. Application of Phylogenetic Networks in Evolutionary Studies. Molecular Biology and Evolution. 2006;23(2):254-67.
42. Tosa Y, Osue J, Eto Y, Oh H-S, Nakayashiki H, Mayama S, et al. Evolution of an avirulence gene, AVR1-CO39, concomitant with the evolution and differentiation of Magnaporthe oryzae. Molecular Plant-Microbe Interactions. 2005;18(11):1148-60.
43. Cesari S, Thilliez G, Ribot C, Chalvon V, Michel C, Jauneau A, et al. The rice resistance protein pair RGA4/RGA5 recognizes the Magnaporthe oryzae effectors AVR-Pia and AVR1-CO39 by direct binding. The Plant cell. 2013;25(4):1463-81. Epub 2013/04/04. doi: 10.1105/tpc.112.107201. PubMed PMID: 23548743; PubMed Central PMCID: PMCPMC3663280.
44. Okuyama Y, Kanzaki H, Abe A, Yoshida K, Tamiru M, Saitoh H, et al. A multifaceted genomics approach allows the isolation of the rice Pia-blast resistance gene consisting of two adjacent NBS-LRR protein genes. The Plant Journal. 2011;66(3):467-79.
45. Weir BS, Cockerham CC. Estimating F-statistics for the analysis of population structure. Evolution. 1984;38:1358-70. PubMed PMID: 283.
46. Hahn MW. Molecular population genetics: Oxford University Press; 2018.
47. Hirata K, Kusaba M, Chuma I, Osue J, Nakayashiki H, Mayama S, et al. Speciation in Pyricularia inferred from multilocus phylogenetic analysis. Mycological Research. 2007;111(7):799-808.
48. Gómez Luciano LB, Tsai IJ, Chuma I, Tosa Y, Chen Y-H, Li J-Y, et al. Blast fungal genomes show frequent chromosomal changes, gene gains and losses, and effector gene turnover. Molecular Biology and Evolution. 2019;36(6):1148-61.
49. Yang Z. Likelihood ratio tests for detecting positive selection and application to primate lysozyme evolution. Molecular biology and evolution. 1998;15(5):568-73.

50. Ortiz D, De Guillen K, Cesari S, Chalvon V, Gracy J, Padilla A, et al. Recognition of the Magnaporthe oryzae effector AVR-Pia by the decoy domain of the rice NLR immune receptor RGA5. The Plant cell. 2017;29(1):156-68.
51. Maqbool A, Saitoh H, Franceschetti M, Stevenson CEM, Uemura A, Kanzaki H, et al. Structural basis of pathogen recognition by an integrated HMA domain in a plant NLR immune receptor. Elife. 2015;4.
52. Guo L, Cesari S, de Guillen K, Chalvon V, Mammri L, Ma M, et al. Specific recognition of two MAX effectors by integrated HMA domains in plant immune receptors involves distinct binding surfaces. Proceedings of the National Academy of Sciences. 2018;115(45):11637-42.
53. Bentham AR, Petit-Houdenot Y, Win J, Chuma I, Terauchi R, Banfield MJ, et al. A single amino acid polymorphism in a conserved effector of the multihost blast fungus pathogen expands host-target binding spectrum. PLoS Pathogens. 2021;17(11):e1009957.
54. Clay K, Kover PX. The Red Queen hypothesis and plant/pathogen interactions. Annual review of Phytopathology. 1996;34(1):29-50.
55. Van Valen L. A new evolutionary law. 1973.
56. Yang Z, Bielawski JP. Statistical methods for detecting molecular adaptation. Trends in ecology & evolution. 2000;15(12):496-503.
57. Kourelis J, Marchal C, Posbeyikian A, Harant A, Kamoun S. NLR immune receptor–nanobody fusions confer plant disease resistance. Science. 2023;379(6635):934-9.
58. Chiapello H, Mallet L, Guerin C, Aguileta G, Amselem J, Kroj T, et al. Deciphering Genome Content and Evolutionary Relationships of Isolates from the Fungus Magnaporthe oryzae Attacking Different Host Plants. Genome Biol Evol. 2015;7(10):2896-912. Epub 2015/10/11. doi: 10.1093/gbe/evv187. PubMed PMID: 26454013; PubMed Central PMCID: PMCPMC4684704.
59. Soyer JL, El Ghalid M, Glaser N, Ollivier B, Linglin J, Grandaubert J, et al. Epigenetic control of effector gene expression in the plant pathogenic fungus Leptosphaeria maculans. PLoS genetics. 2014;10(3):e1004227.
60. Tang B, Yan X, Ryder LS, Cruz-Mireles N, Soanes DM, Molinari C, et al. Rgs1 is a regulator of effector gene expression during plant infection by the rice blast fungus Magnaporthe oryzae. bioRxiv. 2022:2022-09.
61. Fall LA, Salazar MM, Drnevich J, Holmes JR, Tseng M-C, Kolb FL, et al. Field pathogenomics of Fusarium head blight reveals pathogen transcriptome differences due to host resistance. Mycologia. 2019;111(4):563-73.
62. Sonah H, Zhang X, Deshmukh RK, Borhan MH, Fernando WGD, Belanger RR. Comparative transcriptomic analysis of virulence factors in Leptosphaeria maculans during compatible and incompatible interactions with canola. Frontiers in plant science. 2016;7:1784.
63. Arora S, Steed A, Goddard R, Gaurav K, O'Hara T, Schoen A, et al. A wheat kinase and immune receptor form host-specificity barriers against the blast fungus. Nature Plants. 2023:1-8.
64. Farman ML, Eto Y, Nakao T, Tosa Y, Nakayashiki H, Mayama S, et al. Analysis of the structure of the *AVR1-Co39* avirulence locus in virulent rice-infecting isolates of *Magnaporthe grisea*. Molecular Plant-Microbe Interactions. 2002;15:6-16. PubMed PMID: 90.
65. Kang S, Sweigard Ja Fau - Valent B, Valent B. The PWL host specificity gene family in the blast fungus Magnaporthe grisea. Molecular Plant Microbe Interactions. 1995;(0894-0282 (Print)).
66. Brabham HJ, Gómez De La Cruz D, Were V, Shimizu M, Saitoh H, Hernández-Pinzón I, et al. Barley MLA3 recognizes the host-specificity determinant PWL2 from rice blast (M. oryzae). bioRxiv. 2022:2022-10.
67. Thierry M, Charriat F, Milazzo J, Adreit H, Ravel S, Cros-Arteil S, et al. Maintenance of divergent lineages of the Rice Blast Fungus Pyricularia oryzae through niche separation, loss of sex and post-mating genetic incompatibilities. PLoS pathogens. 2022;18(7):e1010687.
68. Martin M. Cutadapt removes adapter sequences from high-throughput sequencing reads. EMBnet journal. 2011;17(1):10-2.
69. Simpson JT, Wong K, Jackman SD, Schein JE, Jones SJM, Birol I. ABySS: a parallel assembler for short read sequence data. Genome research. 2009;19(6):1117-23.
70. Hoff KJ, Lange S, Lomsadze A, Borodovsky M, Stanke M. BRAKER1: unsupervised RNA-Seq-based genome annotation with GeneMark-ET and AUGUSTUS. Bioinformatics. 2015;32(5):767-9.
71. Abascal F, Zardoya R, Telford MJ. TranslatorX: multiple alignment of nucleotide sequences guided by amino acid translations. Nucleic acids research. 2010;38(suppl_2):W7-W13.
72. Katoh K, Toh H. Recent developments in the MAFFT multiple sequence alignment program. Briefings in Bioinformatics. 2008;9(4):286-98. doi: 10.1093/bib/bbn013. PubMed PMID: ISI:000256756400004.

73. Castresana J. Selection of conserved blocks from multiple alignments for their use in phylogenetic analysis. Molecular biology and evolution. 2000;17(4):540-52.
74. Petersen TN, Brunak S, Von Heijne G, Nielsen H. SignalP 4.0: discriminating signal peptides from transmembrane regions. Nature methods. 2011;8(10):785-6.
75. Emanuelsson O, Nielsen H, Brunak S, Von Heijne G. Predicting subcellular localization of proteins based on their N-terminal amino acid sequence. Journal of molecular biology. 2000;300(4):1005-16.
76. Krogh A, Larsson B, Von Heijne G, Sonnhammer ELL. Predicting transmembrane protein topology with a hidden Markov model: application to complete genomes. Journal of molecular biology. 2001;305(3):567-80.
77. Robinson JT, Thorvaldsdóttir H, Turner D, Mesirov JP. igv. js: an embeddable JavaScript implementation of the Integrative Genomics Viewer (IGV). Bioinformatics. 2023;39(1):btac830.
78. Robinson JT, Thorvaldsdóttir H, Winckler W, Guttman M, Lander ES, Getz G, et al. Integrative genomics viewer. Nature biotechnology. 2011;29(1):24-6.
79. Webb B, Sali A. Protein Structure Modeling with MODELLER. Methods Mol Biol. 2021;2199(1940-6029 (Electronic)):239–55.
80. Zhou H, Zhou Y. Distance-scaled, finite ideal-gas reference state improves structure-derived potentials of mean force for structure selection and stability prediction. Protein science. 2002;11(11):2714-26.
81. Zhou H, Skolnick J. GOAP: a generalized orientation-dependent, all-atom statistical potential for protein structure prediction. Biophysical journal. 2011;101(8):2043-52.
82. Benkert P, Tosatto SCE, Schomburg D. QMEAN: A comprehensive scoring function for model quality assessment. Proteins: Structure, Function, and Bioinformatics. 2008;71(1):261-77.
83. Schrödinger L, DeLano W. PyMOL. 2020.
84. Tajima F. Evolutionary relationship of DNA sequences in finite populations. Genetics. 1983;105(2):437-60.
85. Siol M, Coudoux T, Ravel S, De Mita S. EggLib 3: A python package for population genetics and genomics. Molecular Ecology Resources. 2022;22(8):3176-87.
86. Slater GSC, Birney E. Automated generation of heuristics for biological sequence comparison. BMC bioinformatics. 2005;6(1):1-11.
87. Yang Z. PAML: a program package for phylogenetic analysis by maximum likelihood. Computer applications in the biosciences. 1997;13(5):555-6.
88. Villalba F, Collemare J, Landraud P, Lambou K, Brozek V, Cirer B, et al. Improved gene targeting in Magnaporthe grisea by inactivation of MgKU80 required for non-homologous end joining. Fungal Genetics and Biology. 2008;45(1):68-75.
89. Ribot C, Césari S, Abidi I, Chalvon V, Bournaud C, Vallet J, et al. The M agnaporthe oryzae effector AVR 1–CO 39 is translocated into rice cells independently of a fungal-derived machinery. The Plant Journal. 2013;74(1):1-12.
90. Pélissier R, Buendia L, Brousse A, Temple C, Ballini E, Fort F, et al. Plant neighbour-modulated susceptibility to pathogens in intraspecific mixtures. Journal of experimental botany. 2021;72(18):6570-80.
91. Frishman D, Argos P. Knowledge-based protein secondary structure assignment. Proteins: Structure, Function, and Bioinformatics. 1995;23(4):566-79.

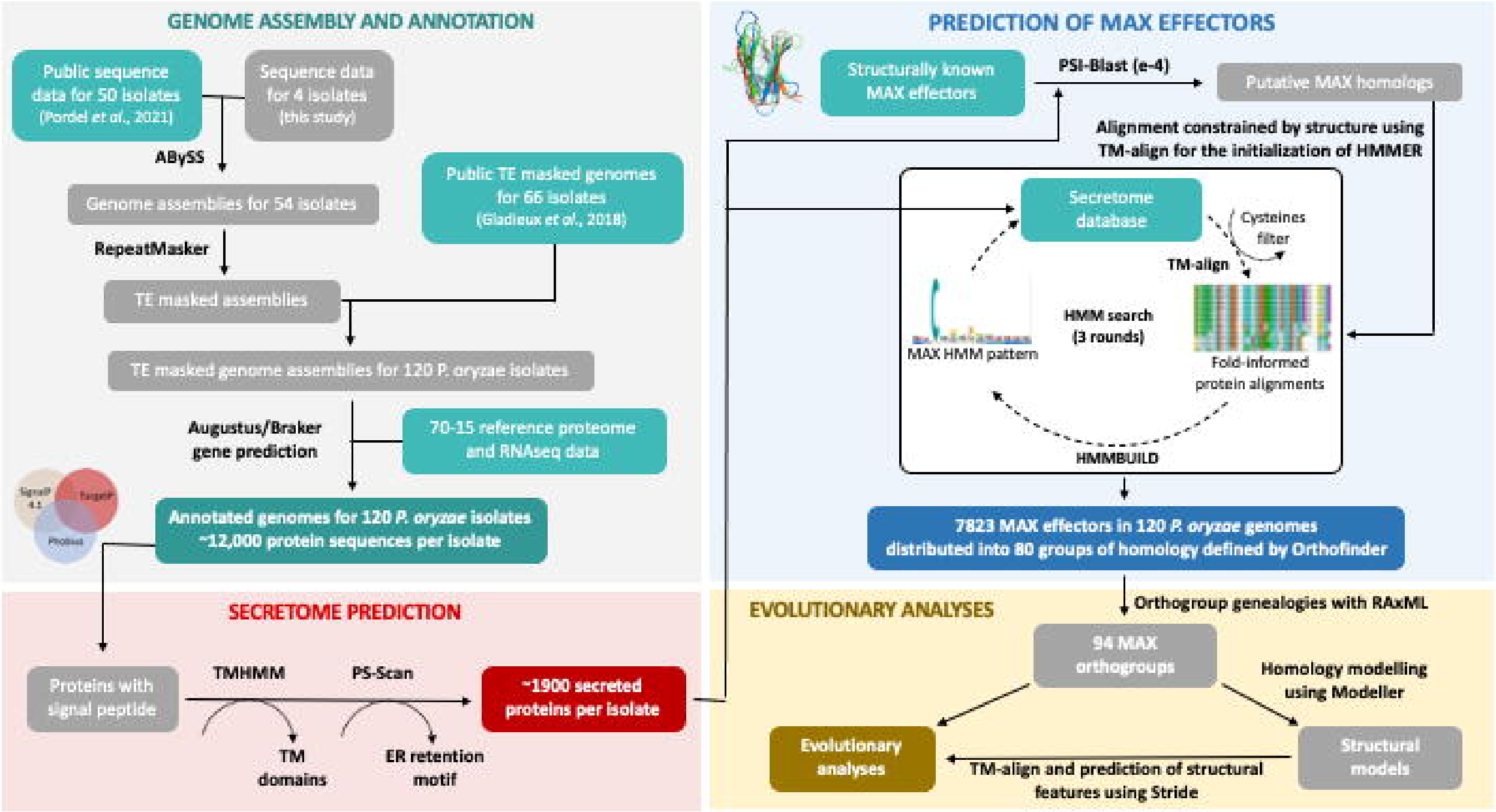
GENOME ASSEMBLY AND ANNOTATION
Public sequence data for 50 isolates (Pordel et al., 2021)
Sequence data for 4 isolates (this study)
ABySS
Genome assemblies for 54 isolates
Public TE masked genomes for 66 isolates (Gladieux et al., 2018)
RepeatMasker
TE masked assemblies
TE masked genome assemblies for 120 P. oryzae isolates
Augustus/Braker gene prediction
70-15 reference proteome and RNAseq data
Annotated genomes for 120 P. oryzae isolates ~12,000 protein sequences per isolate
SECRETOME PREDICTION
Proteins with signal peptide
TMHMM
PS-Scan
~1900 secreted proteins per isolate
TM domains
ER retention motif
PREDICTION OF MAX EFFECTORS
Structurally known MAX effectors
PSI-Blast (e-4)
Putative MAX homologs
Alignment constrained by structure using TM-align for the initialization of HMMER
Secretome database
Cysteines filter
TM-align
MAX HMM pattern
HMM search (3 rounds)
Fold-informed protein alignments
HMMBUILD
7823 MAX effectors in 120 P. oryzae genomes distributed into 80 groups of homology defined by Orthofinder
EVOLUTIONARY ANALYSES
Orthogroup genealogies with RAxML
94 MAX orthogroups
Homology modelling using Modeller
Evolutionary analyses
TM-align and prediction of structural features using Stride
Structural models

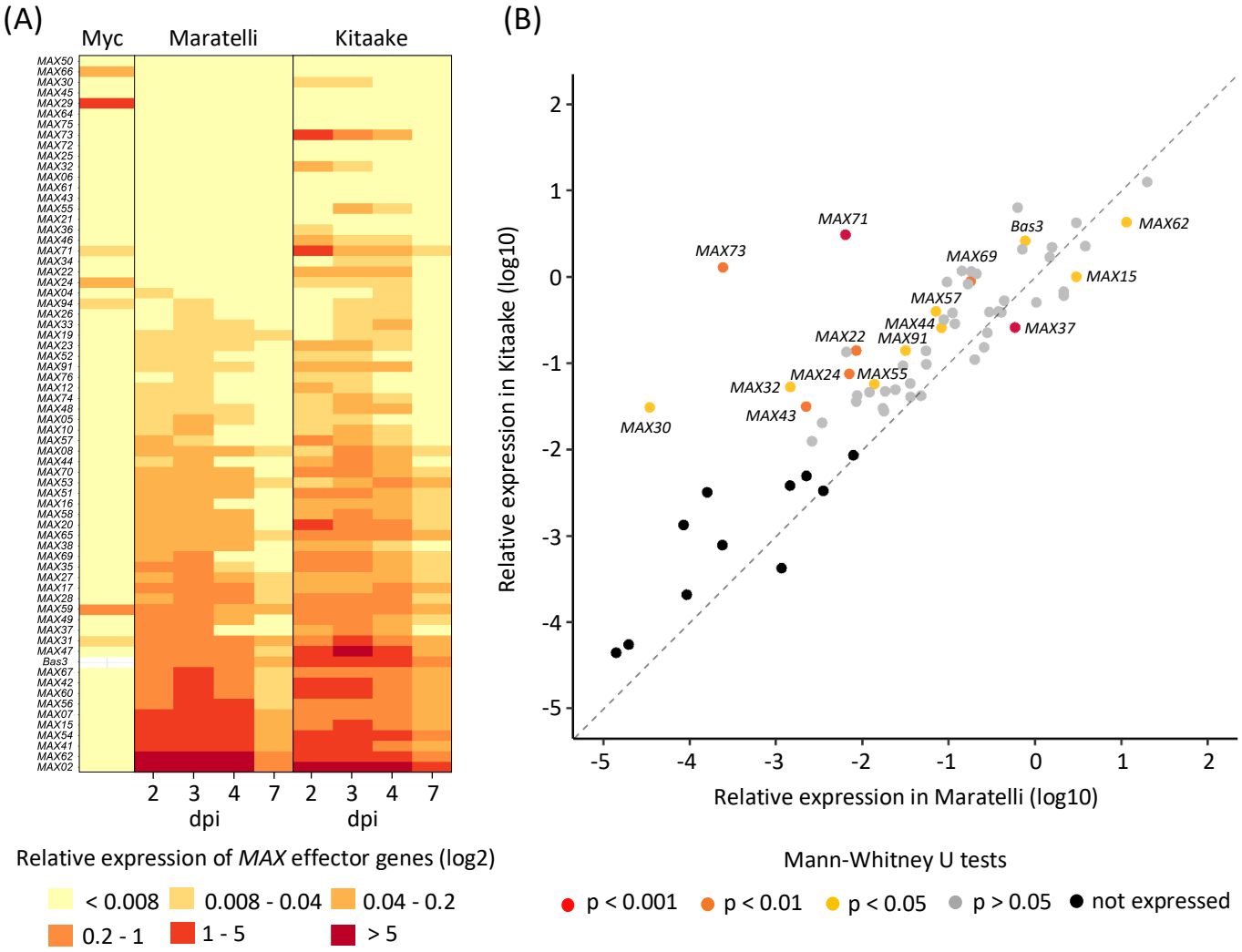
(A)
Myc
Maratelli
Kitaake
MAX50
MAX66
MAX30
MAX45
MAX29
MAX64
MAX75
MAX73
MAX72
MAX25
MAX32
MAX06
MAX61
MAX43
MAX55
MAX21
MAX36
MAX46
MAX71
MAX34
MAX22
MAX24
MAX04
MAX94
MAX26
MAX33
MAX19
MAX23
MAX52
MAX91
MAX76
MAX12
MAX74
MAX48
MAX05
MAX10
MAX57
MAX08
MAX44
MAX70
MAX53
MAX51
MAX16
MAX58
MAX20
MAX65
MAX38
MAX69
MAX35
MAX27
MAX17
MAX28
MAX59
MAX49
MAX37
MAX31
MAX47
Bas3
MAX67
MAX42
MAX60
MAX56
MAX07
MAX15
MAX54
MAX41
MAX62
MAX02
2 3 4 7 2 3 4 7
dpi dpi
Relative expression of MAX effector genes (log2)
< 0.008
0.008 - 0.04
0.04 - 0.2
0.2 - 1
1 - 5
> 5
(B)
Relative expression in Kitaake (log10)
Relative expression in Maratelli (log10)
MAX71
MAX73
Bas3
MAX62
MAX69
MAX15
MAX57
MAX44
MAX37
MAX22
MAX91
MAX24
MAX55
MAX32
MAX43
MAX30
Mann-Whitney U tests
p < 0.001
p < 0.01
p < 0.05
p > 0.05
not expressed

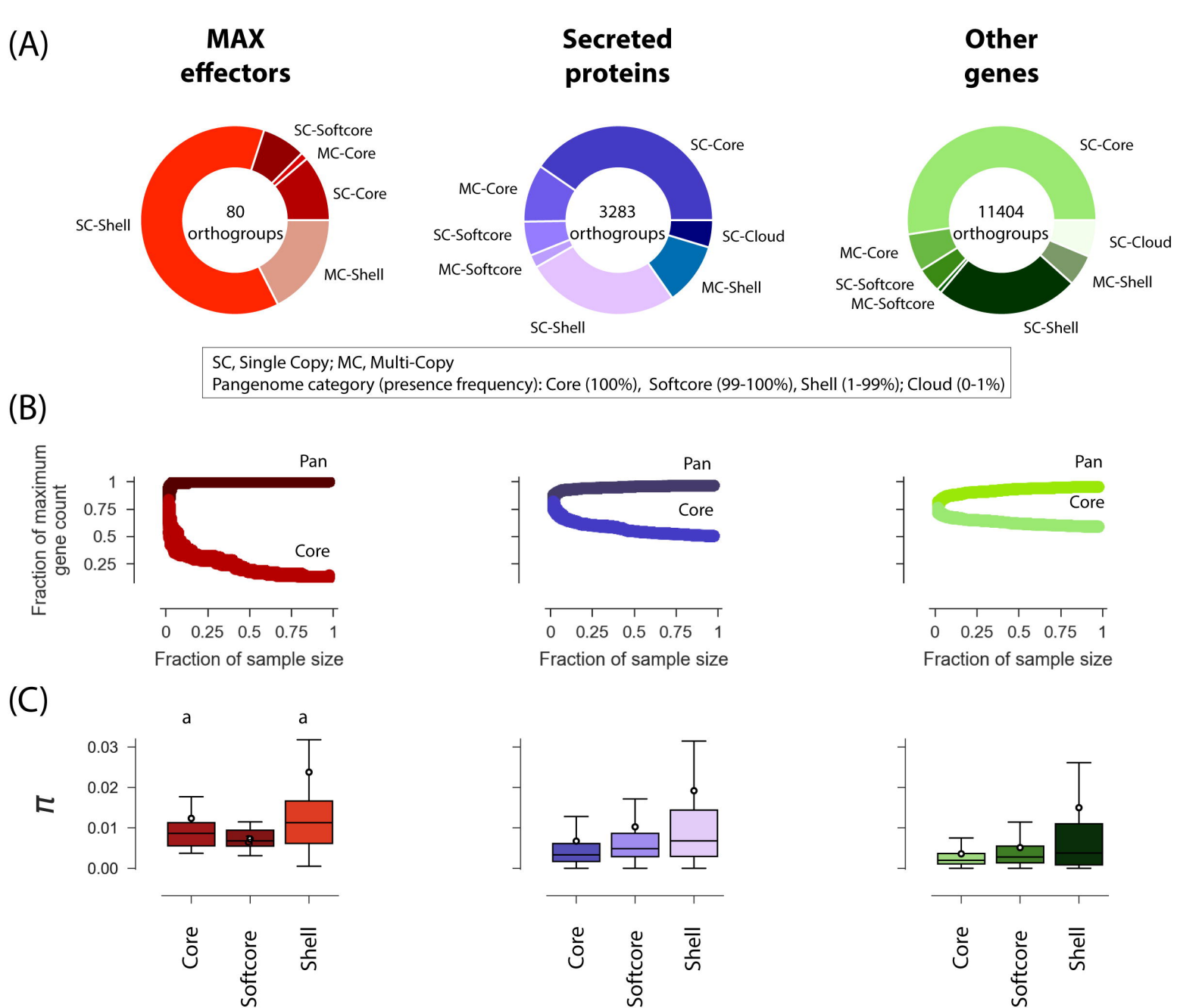
(A)
MAX effectors
Secreted proteins
Other genes
80 orthogroups
SC-Softcore
MC-Core
SC-Core
SC-Shell
MC-Shell
3283 orthogroups
SC-Core
MC-Core
SC-Softcore
MC-Softcore
SC-Cloud
MC-Shell
SC-Shell
11404 orthogroups
SC-Core
SC-Cloud
MC-Core
SC-Softcore
MC-Softcore
MC-Shell
SC-Shell
SC, Single Copy; MC, Multi-Copy
Pangenome category (presence frequency): Core (100%), Softcore (99-100%), Shell (1-99%); Cloud (0-1%)
(B)
Fraction of maximum gene count
Pan
Core
Fraction of sample size
(C)
π
a
a
Core
Softcore
Shell

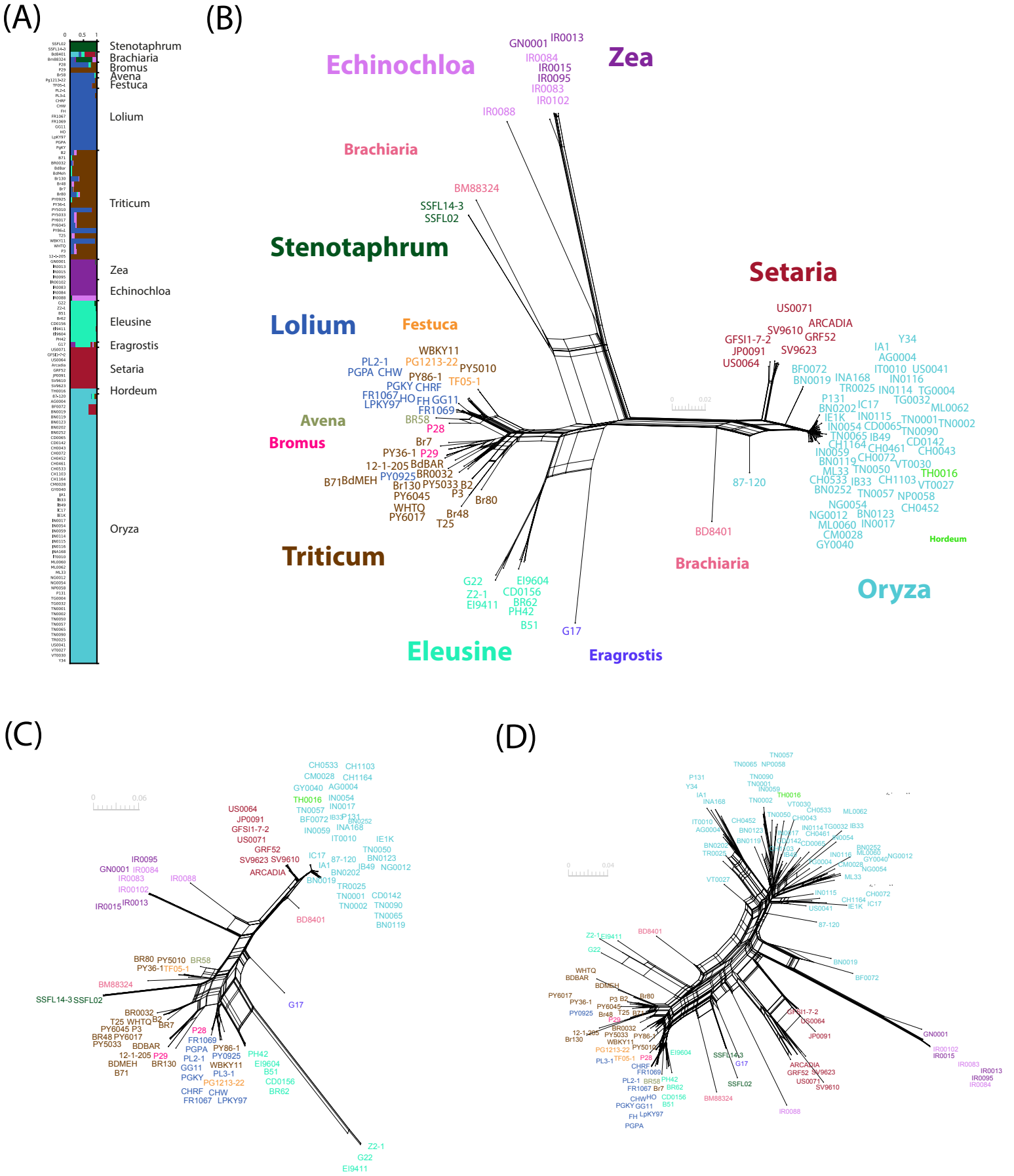
(A)
Stenotaphrum
Brachiaria
Bromus
Avena
Festuca
Lolium
Triticum
Zea
Echinochloa
Eleusine
Eragrostis
Setaria
Hordeum
Oryza
(B)
Echinochloa
Zea
Brachiaria
Stenotaphrum
Setaria
Lolium
Festuca
Avena
Bromus
Triticum
Eleusine
Eragrostis
Hordeum
Oryza
(C)
(D)

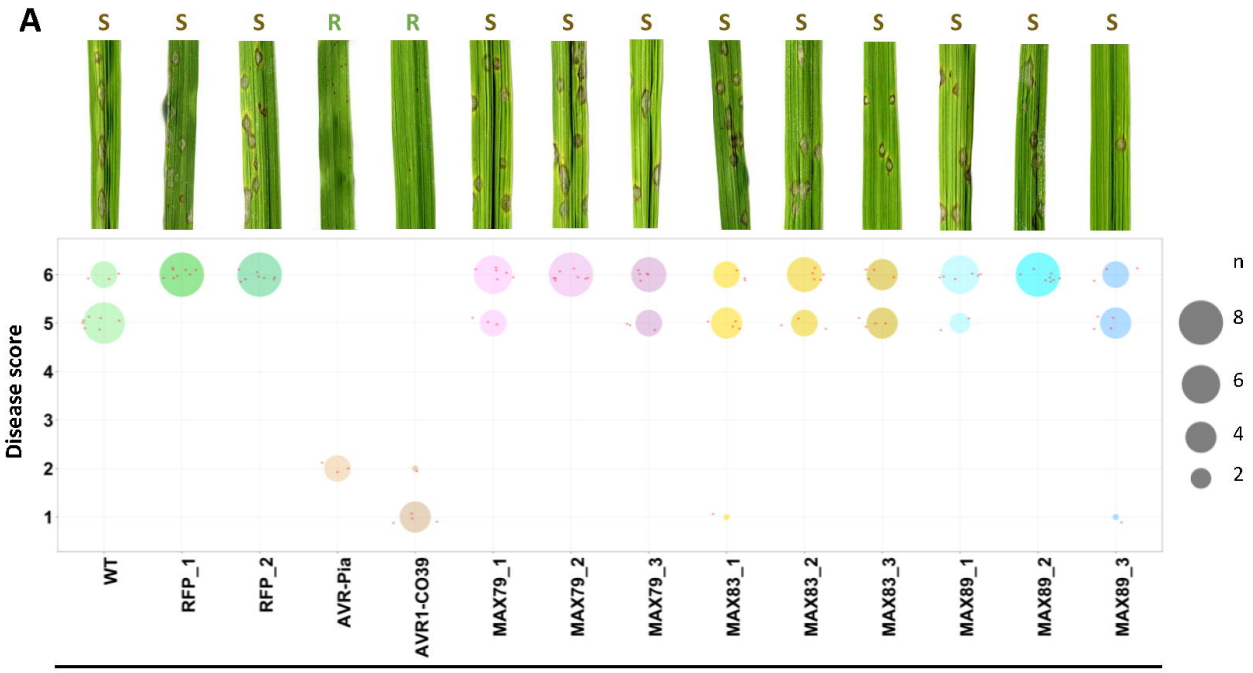

Aichi Asahi plants (*Pia+*) inoculated with Guy11

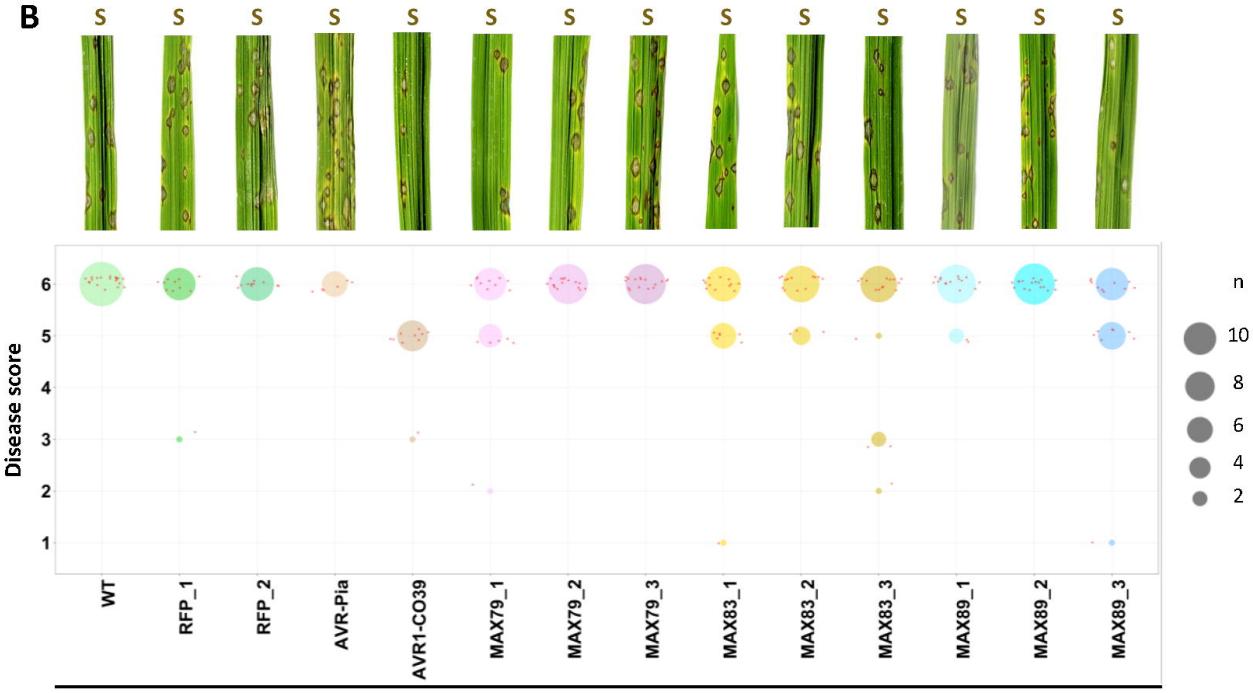

Nipponbare plants (*pia-*) inoculated with Guy11

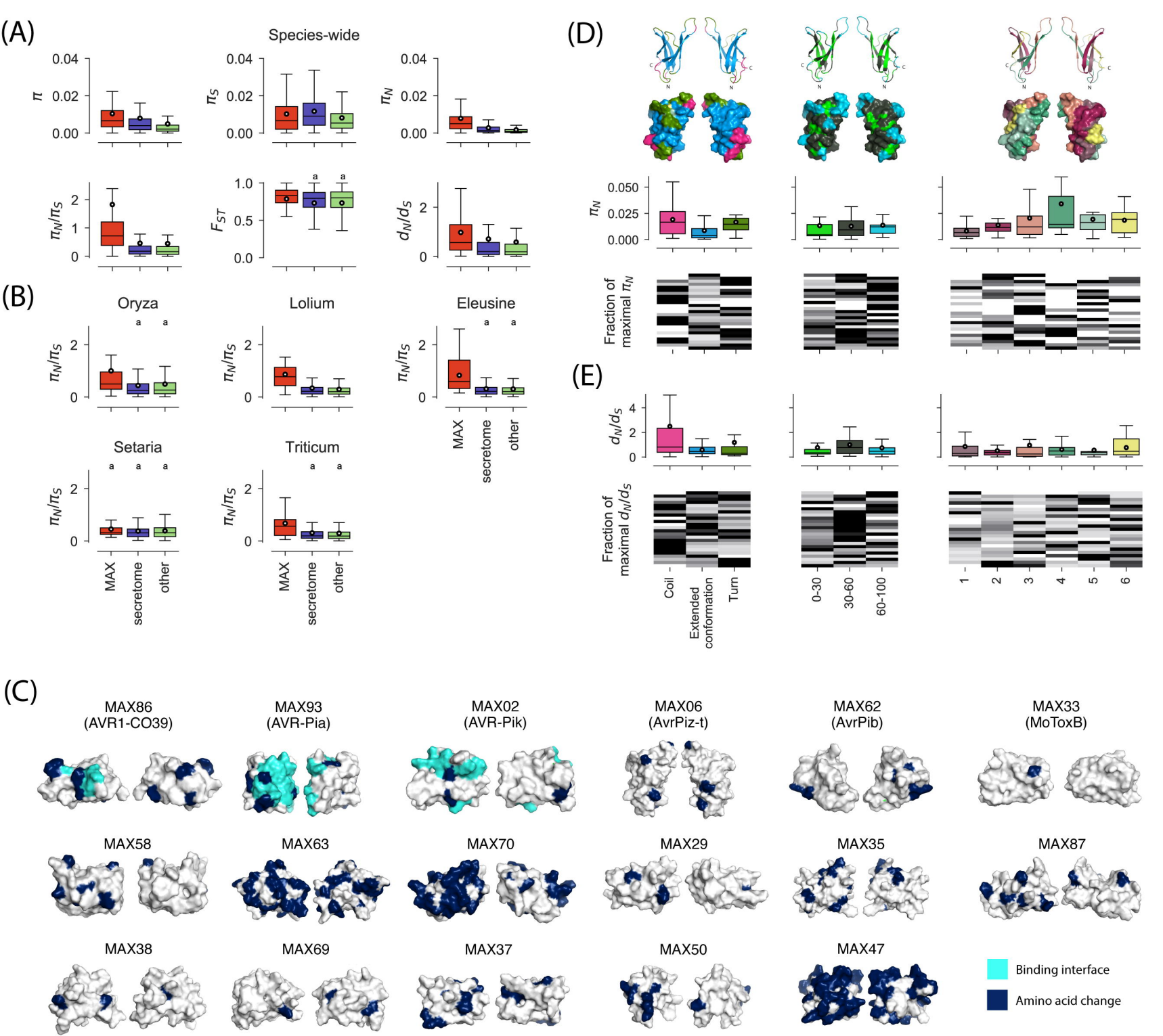
(A)
Species-wide
π
π_S
π_N
π_N/π_S
F_{ST}
d_N/d_S
(B)
Oryza
Lolium
Eleusine
Setaria
Triticum
MAX
secretome
other
(C)
MAX86 (AVR1-CO39)
MAX93 (AVR-Pia)
MAX02 (AVR-Pik)
MAX06 (AvrPiz-t)
MAX62 (AvrPib)
MAX33 (MoToxB)
MAX58
MAX63
MAX70
MAX29
MAX35
MAX87
MAX38
MAX69
MAX37
MAX50
MAX47
Binding interface
Amino acid change
(D)
Fraction of maximal π_N
(E)
Fraction of maximal d_N/d_S
Coil
Extended conformation
Turn
0-30
30-60
60-100
1
2
3
4
5
6